National Library of Canada
Acquisitions and Bibliographic Services Branch
395 Wellington Street
Ottawa, Ontario
K1A 0N4

Bibliothèque nationale du Canada
Direction des acquisitions et des services bibliographiques
395, rue Wellington
Ottawa (Ontario)
K1A 0N4

Your file Votre référence

Our file Notre référence

NOTICE

The quality of this microform is heavily dependent upon the quality of the original thesis submitted for microfilming. Every effort has been made to ensure the highest quality of reproduction possible.

If pages are missing, contact the university which granted the degree.

Some pages may have indistinct print especially if the original pages were typed with a poor typewriter ribbon or if the university sent us an inferior photocopy.

Reproduction in full or in part of this microform is governed by the Canadian Copyright Act, R.S.C. 1970, c. C-30, and subsequent amendments.

AVIS

La qualité de cette microforme dépend grandement de la qualité de la thèse soumise au microfilmage. Nous avons tout fait pour assurer une qualité supérieure de reproduction.

S'il manque des pages, veuillez communiquer avec l'université qui a conféré le grade.

La qualité d'impression de certaines pages peut laisser à désirer, surtout si les pages originales ont été dactylographiées à l'aide d'un ruban usé ou si l'université nous a fait parvenir une photocopie de qualité inférieure.

La reproduction, même partielle, de cette microforme est soumise à la Loi canadienne sur le droit d'auteur, SRC 1970, c. C-30, et ses amendements subséquents.

Canada

UNIVERSITY OF ALBERTA

A FINITE ELEMENT MODEL OF THE RIB CAGE

by

© JANINE M. THOMPSON

A thesis submitted to the Faculty of Graduate Studies and Research in partial fulfilment of the requirements for the degree of Master of Science.

Department of Mechanical Engineering

Edmonton, Alberta
FALL 1995

National Library of Canada
Acquisitions and Bibliographic Services Branch
395 Wellington Street
Ottawa, Ontario
K1A 0N4

Bibliothèque nationale du Canada
Direction des acquisitions et des services bibliographiques
395, rue Wellington
Ottawa (Ontario)
K1A 0N4

Your file Votre référence

Our file Notre référence

THE AUTHOR HAS GRANTED AN IRREVOCABLE NON-EXCLUSIVE LICENCE ALLOWING THE NATIONAL LIBRARY OF CANADA TO REPRODUCE, LOAN, DISTRIBUTE OR SELL COPIES OF HIS/HER THESIS BY ANY MEANS AND IN ANY FORM OR FORMAT, MAKING THIS THESIS AVAILABLE TO INTERESTED PERSONS.

L'AUTEUR A ACCORDE UNE LICENCE IRREVOCABLE ET NON EXCLUSIVE PERMETTANT A LA BIBLIOTHEQUE NATIONALE DU CANADA DE REPRODUIRE, PRETER, DISTRIBUER OU VENDRE DES COPIES DE SA THESE DE QUELQUE MANIERE ET SOUS QUELQUE FORME QUE CE SOIT POUR METTRE DES EXEMPLAIRES DE CETTE THESE A LA DISPOSITION DES PERSONNE INTERESSEES.

THE AUTHOR RETAINS OWNERSHIP OF THE COPYRIGHT IN HIS/HER THESIS. NEITHER THE THESIS NOR SUBSTANTIAL EXTRACTS FROM IT MAY BE PRINTED OR OTHERWISE REPRODUCED WITHOUT HIS/HER PERMISSION.

L'AUTEUR CONSERVE LA PROPRIETE DU DROIT D'AUTEUR QUI PROTEGE SA THESE. NI LA THESE NI DES EXTRAITS SUBSTANTIELS DE CELLE-CI NE DOIVENT ETRE IMPRIMES OU AUTREMENT REPRODUITS SANS SON AUTORISATION.

ISBN 0-612-06546-4

Canada

UNIVERSITY OF ALBERTA

LIBRARY RELEASE FORM

NAME OF AUTHOR: Janine M. Thompson

TITLE OF THESIS: A Finite Element Model of the Rib Cage

DEGREE: Master of Science

YEAR THIS DEGREE GRANTED: 1995

Permission is hereby granted to the University of Alberta Library to reproduce single copies of this thesis and to lend or sell such copies for private, scholarly, or scientific research purposes only.

The author reserves all other publication and other rights in association with the copyright in the thesis, and except as hereinbefore provided neither the thesis nor any substantial portion thereof may be printed or otherwise reproduced in any material form whatever without the author's prior written permission.

Janine Thompson

5465 Braesvalley #548
Houston, Texas
USA 77096

Date: 23 May 1995

UNIVERSITY OF ALBERTA

FACULTY OF GRADUATE STUDIES AND RESEARCH

The undersigned certify that they have read, and recommend to the Faculty of Graduate Studies and Research for acceptance, a thesis entitled A Finite Element Model of the Rib Cage submitted by Janine M. Thompson in partial fulfilment of the requirements for the degree of Master of Science.

Dr. David Budney -- Co-Supervisor

Dr. Ken Fyfe

Dr. Terry Hrudey

Jim Raso -- Co-Supervisor

May 17, 1995

For James

ABSTRACT

Scoliosis is an abnormal curvature of the spine with associated vertebral rotation. Bracing attempts to realign the spine through the use of pressure pads which transmit corrective forces through the ribs to the spine. The complex articulations between the ribs and the vertebrae are crucial elements in achieving successful force transmission. An understanding of the kinematics of the rib cage, particularly these articulations, would improve the effectiveness of non-operative management of scoliosis. A finite element model has been developed to study this brace-body interaction. The three thoracic vertebrae, two sets of rib pairs, and the corresponding section of the sternum, along with the associated soft tissues, ligaments, and intervertebral discs, have been modelled. A detailed, physiologically correct model of the rib-vertebra articulation has also been incorporated.

The model is used to determine the qualitative effects of bracing on the rib cage. A parametric study of the articulation ligaments was performed wherein the stiffness values of each set of ligaments was varied according to published data. Different boundary conditions were investigated to create the most physiologically accurate model. The applied brace loading created movements of the vertebrae which are desirable in correcting scoliosis. The ligaments of the rib-vertebra articulations have a major role in determining these vertebral displacements. Stiffness values for these ligaments may be varied over a large range without substantially affecting the output of the model. Boundary conditions which accurately mimic physiological conditions are necessary to obtain reliable model output.

ACKNOWLEDGEMENTS

The author wishes to acknowledge and thank the following individuals whose contributions enabled the completion of this project.

Jim Raso of the Glenrose Rehabilitation Hospital and Dr. Dave Budney of the University of Alberta for their supervision and guidance throughout the entire project. Doug Hill, also of the Glenrose Rehabilitation Hospital, both for his computer expertise and his patience with my computer illiteracy. A thank you is also in order for all the graduate students at the Glenrose Rehabilitation Hospital whose knowledge of the inner workings of the computer systems was invaluable.

I'd like also to thank Ron Shute for his prior finite element models of the spine and for teaching me the intricacies of the ALGOR Finite Element Analysis Package. The many consultations with Dr. Terry Hrudey and Dr. Tai Wong concerning finite element modelling procedures during this project were also greatly appreciated.

On a personal note, thank you to my parents, Bill and Rosie Babowal, for letting me stay with them, thank you to my husband James for all his support, and thank you to Alexandra whose birth provided the motivation to finish this thesis.

TABLE OF CONTENTS

Chapter One: Introduction....1

1.0 Introduction....1

1.0.1 Challenges of Modelling the Spine and Rib Cage....1

1.0.2 Objectives of this Study....2

1.0.3 Details of Chapters....3

1.1 Anatomy of the Spine and the Rib Cage....3

1.1.1 Anatomy of the Vertebral Column....3

1.1.2 Anatomy of the Vertebra....3

1.1.3 Anatomy of the Intervertebral Discs....4

1.1.4 Ligaments of the Vertebral Column....5

1.1.5 Anatomy of the Rib Cage....5

1.2 Coordinate System....6

1.3 Scoliosis....7

1.3.1 Anatomy of Scoliosis....7

1.3.2 Treatment of Scoliosis....8

1.4 Anatomy and Biomechanics of the Articulations....8

1.4.1 Costo-vertebral Articulation....8

1.4.2 Costo-transverse Articulation....9

1.4.3 Costo-sternal Articulation....10

1.5 Mechanical Behavior of Biological Tissues....10

1.5.1 Collagen....10

1.5.2 Ligaments....11

1.6 Biomechanics of the Spine and Rib Cage....11

1.6.1 The Ribs....11

1.6.2 Costal Cartilage....12

1.6.3 Intervertebral Discs....12

Chapter Two: Literature Review....21
2.0 Overview of the Literature Review....21
2.1 Roberts and Chen....22
2.2 Schultz, Belytschko, and Andriacchi....23
2.3 Andriacchi, Schultz, Belytschko, and Galante....24
2.4 Closkey, Schultz, and Luchies....25
2.5 Sundaram and Feng....26
2.6 Stokes and Laible....27
2.7 Material Properties....27

Chapter Three: Model Description....29
3.0 Proposed Model....29
3.0.1 Model Components....29
3.0.2 Element Types....30
3.0.3 Non-linear Ligament Behaviour....31
3.1 Geometric Description....31
3.1.1 Rib Data....31
3.1.2 Articulation Geometry....32
3.1.3 Sternum and Vertebrae....33
3.2 Material Properties....34
3.2.1 Cortical Bone....34
3.2.2 Rib Material Properties....34
3.2.3 Spinal Ligaments....35
3.2.4 Costo-transverse and Costo-vertebral Articulations....36
3.2.5 Costal Cartilage....37
3.2.6 Intercostal Membranes....38
3.2.7 Intervertebral Discs....38

3.3 Applied Loading....39
3.4 Boundary Conditions....39

Chapter Four: Results....51
4.0 Introduction to Chapter Four....51
4.1 Validation of the Model....51
4.2 Initial Studies of the Model....53
4.2.1 Ligament Study....54
4.2.2 Boundary Condition Study....55
4.3 Output Parameters....55
4.4 Results....56
4.4.1 General Results....56
4.4.2 Ligament Study Results....56
4.4.3 Boundary Condition Study Results....57
4.4.4 Discussion of Figures....57

Chapter Five: Discussion of Results....65
5.0 General Qualitative Results....65
5.1 Parametric Study....66
5.1.1 Articulation Ligaments....66
5.1.2 Costal Cartilage....67
5.1.3 Intercostal Membranes....68
5.2 Boundary Condition Study....68

Chapter Six: Limitations and Future Work....70
6.0 Conclusions....70
6.1 Limitations....71
6.2 Future Work....72
References....74

LIST OF TABLES

Table 1: Material Properties and Stiffness Values from the Literature.....28

Table 2: Material Properties of Spinal Ligament Elements.....35

Table 3: Stiffness Values for the Ligaments of the Rib-Vertebra Articulations.....37

Table 4: Stiffness Values for the Costal Cartilage Elements.....38

Table 5: Intervertebral Disc Stiffness Parameters.....39

Table 6: Summary of Input Parameter Changes.....54

Table 7: Percentage Variations for the Ligament Study (mean values).....67

LIST OF FIGURES

Figure 1: The Vertebral Column....13

Figure 2: Components of the Vertebra....14

Figure 3: The Intervertebral Disc....14

Figure 4: Ligaments of the Spinal Column....15

Figure 5: The Rib Cage....16

Figure 6: Components of the Rib....17

Figure 7: The Coordinate System....18

Figure 8: Movement of the Rib-Vertebra Articulation....19

Figure 9: Ligaments of the Costo-vertebral Articulation....20

Figure 10: Ligaments of the Costo-transverse Articulation....20

Figure 11: Side View of the Model....41

Figure 12: Isometric View of the Model Ribs and Intercostal Membranes....42

Figure 13: Plan View of the Model....43

Figure 14: Expanded View of the Rib-Vertebra Articulation....44

Figure 15: Isometric View of the Ligaments of the Rib-Vertebra Articulation....45

Figure 16: Validation of Rib Elements....46

Figure 17: Stress-Strain Relationship for the Supraspinous Ligament....47

Figure 18: Validation of the Ligaments of the Rib-Vertebra Articulation....48

Figure 19: Validation of the Costal Cartilage Elements....49

Figure 20: Boundary Intercostal Membranes at Physiological Length....50

Figure 21: Boundary Intercostal Membranes at Extended Length....50

Figure 22: Validation of Model....59

Figure 23: Vertebral Rotations in the Frontal Plane due to Brace Loading....60

Figure 24: Vertebral Rotations in the Horizontal Plane due to Brace Loading....61

Figure 25: Changes in Rib Cage Diameters....62

Figure 26: Rib Displacements at the Point of Load Application.....62

Figure 27: Rib Displacements at the Costo-vertebral Articulation.....63

Figure 28: Displacements at the Centre Front of the Vertebrae.....63

Figure 29: Vertebral Rotations.....64

GLOSSARY

ANNULUS FIBROSUS: concentric bands of fibres found within the intervertebral discs.

CANCELLOUS BONE: spongy bone with a lattice structure.

CARTILAGE: a fibrous connective tissue.

CERVICAL: the region of the neck.

COLLAGEN: the fibrous protein which is the main structural component of bones, ligaments, tendons, cartilage, skin, and all other connective tissues.

CORTICAL BONE: compact bone that is hard and dense.

COSTAL CARTILAGES: cartilage sections connecting the first seven ribs to the sternum.

COSTO-TRANSVERSE ARTICULATION: site of articulation between the tubercle of the rib and the transverse process of the vertebra.

COSTO-VERTEBRAL ARTICULATION: site of articulation between the head of the rib and the vertebral body.

DORSAL: Situated on or directed toward the back surface. Opposite of ventral.

ENDPLATES: cartilage structure located between the vertebral bodies and the adjacent intervertebral discs.

FACETS: Small plane surfaces or depressions on the bones (the vertebrae and the ribs).

FASCIA: A sheet of fibrous tissue. The intercostal fascia covers the intercostal muscles.

HYALINE CARTILAGE: flexible, semi-transparent cartilage.

INTERCOSTAL MEMBRANES: the connective tissues and fascia located in the spaces between the ribs.

INTERVERTEBRAL DISCS: the cartilage structures located between adjacent vertebrae.

KYPHOSIS: a spinal curvature which is convex posteriorly.

LIGAMENTS: fibrous bands of elastin and collagen which connect bones and cartilage. Ligaments also serve to strengthen joints.

ANTERIOR LONGITUDINAL: traverses the anterior surfaces of the vertebrae from C1 to the sacrum.

ARTICULAR CAPSULE: extends perpendicularly from facets in the vertebrae, the costo-transverse articulation, and the costo-vertebral articulation.

INTEROSSEOUS COSTO-TRANSVERSE: connects the dorsal surface of the rib neck to the inferior transverse process.

INTRAARTICULAR: located in the interior of the costo-vertebral articulation. This ligament connects the middle of the rib head to the intervertebral disc.

INTRASPINOUS: connects adjacent spinous processes.

LIGAMENTUM FLAVUM: connects the lamina of adjacent vertebrae.

RADIATE: extend from the rib head to the corresponding vertebrae and intervertebral disc.

POSTERIOR COSTO-TRANSVERSE: extends from the tubercle of the rib to the inferior transverse process.

POSTERIOR LONGITUDINAL: traverses the posterior surfaces of the vertebrae from C1 to the sacrum.

SUPERIOR COSTO-TRANSVERSE: extends from the rib neck to the superior transverse process.

SUPRASPINOUS: connects the tips of adjacent spinous processes.

LORDOSIS: a spinal curvature which is concave posteriorly.

LUMBAR SPINE: the section of the spine between the ribs and the sacrum.

MIDAXILLARY LINE: An imaginary line running down the surface of the trunk from the armpit.

NUCLEUS PULPOSUS: the gelatinous core of the intervertebral disc.

PEDICLES: bony projections connecting the body of the vertebrae to the neural arch.

RIB CAGE: the osseocartilaginous cage consisting of the ribs, the sternum, and the spine.

RIBS: the arc-like bones extending from the thoracic vertebrae to the sternum.

RIB-VERTEBRA ARTICULATION: the costo-transverse and the costo-vertebral articulations.

SACRUM: triangular bone located at the base of the spine.

SCOLIOSIS: an abnormal lateral curvature of the spine.

SPINE: the bony structure, extending from the head to the sacrum, which supports the head and the trunk. Also called the vertebral column.

SPINOUS PROCESS: dorsal, bony projections from the posterior of the vertebrae.

STERNUM: the elongated bone located at the middle front of the thorax.

THORACIC SPINE: the region of the spine to which the ribs attach.

THORAX: the chest.

TRANSVERSE PROCESS: lateral, bony projections from the posterior of the vertebrae.

VENTRAL: Situated on or directed to the front or belly surface. Opposite of dorsal.

VERTEBRA: the bony structural segments of the spine.

VISCERAL: Pertaining to the large interior organs of the body.

CHAPTER ONE: INTRODUCTION

1.0 INTRODUCTION

Bracing is a common method of treating scoliosis in adolescents. Pressure pads are placed in various locations within the brace to apply pressures on the trunk. These pressures, which are transmitted through the ribs to the spine, attempt to correct the spinal curvature. However, the exact mechanism of this force transmittal, especially at the rib-vertebra interface, is poorly understood. Knowledge of these complex interactions between the brace, the rib cage, and the spine would result in more effective pressure pad placement and brace treatment.

1.0.1 CHALLENGES OF MODELLING THE SPINE AND RIB CAGE

Several global models, which are outlined in Chapter two, have attempted to represent the entire human thorax using either finite element or mathematical modelling techniques [3, 6, 16, 22, 23]. Many experimental studies have been performed and detailed models developed of the human lumbar spine [10]. Many of the rib cage models have highlighted the significance of the role of the rib-vertebra articulations in rib cage kinematics [3, 6, 16, 22]. However presently, there is a lack of local, detailed models of this articulation. There is a need to develop an anatomically and mechanically accurate model of the costo-transverse and costo-vertebral articulations which incorporates both the ligamentous and kinematic constraints of these joints.

Global models of the entire spine and rib cage would be complex and extensive in terms of their components, geometry, and material properties. In order to create a manageable global model, simplifications in anatomical positioning and biomechanical behaviour must be incorporated. To avoid excessive oversimplification in a global model, a smaller model must first be developed to study the effect of individual components on overall model behaviour. With the knowledge, correct simplifications in model components may be determined.

1.0.2 OBJECTIVES OF THIS STUDY

The objective of this study was to develop and validate a three-dimensional, finite-element model of three vertebrae and two pairs of ribs. Included in this model are detailed representations of both the costo-vertebral and the costo-transverse junctions. This model is the first step in developing a three-dimensional, finite element model of the entire thorax which can then be used to study both the effect of bracing on the trunk and the optimisation of corrective forces.

The objectives of this preliminary model were to:

1. Investigate the mechanics of the transmission of forces from the ribs to the spine,
2. Study the effect of brace forces on the ribs and the spine,
3. Conduct a parametric study of the stiffness values associated with the costo-vertebral, costo-transverse, and costo-sternal articulations, and
4. Investigate the effects of boundary conditions on the output of the model.

1.0.3 DETAILS OF CHAPTERS

This first chapter presents an introduction to the thesis project as well as an overview of the relevant anatomy and biomechanics. Chapter two consists of a literature review of previous finite element and mathematical models of the spine and rib cage. A detailed description of the present model is outlined in Chapter three. Chapter four summarises the validation and testing results of the model. A discussion of these results along with the conclusions of the study, follow in Chapter five. Finally, Chapter six discusses the limitations of this model and offers suggestions for future work in this area.

1.1 ANATOMY OF THE SPINE AND THE RIB CAGE

1.1.1 ANATOMY OF THE VERTEBRAL COLUMN

The vertebral column, shown in Figure 1, is the bony structure extending from the head to the sacrum which supports the head and the trunk. The spine is divided into three regions: the cervical or neck area, the thoracic section to which the ribs attach, and the lumbar region located between the ribs and the sacrum. These sections contain 7, 12, and 5 vertebrae respectively. The vertebrae are separated by intervertebral discs composed of fibrocartilaginous tissue. The vertebral canal, a hollow opening traversed by the spinal cord, spans the length of the vertebral column.

1.1.2 ANATOMY OF THE VERTEBRA

Each vertebra may be separated into two main components: the body and the neural arch. The following components of the vertebra are illustrated in Figure 2. The ventral component of the vertebra, the body, is a cylindrically-shaped, cancellous bone core

covered by a thin cortical bone shell. The top and bottom surfaces of the body, the endplates, serve as attachment sites for the intervertebral discs. The neural arch also has a cancellous bone core with a thicker cortical bone covering. The transverse processes are lateral projections and the spinous processes are dorsal projections both from the posterior of the vertebra. The pedicles are dorsal projections connecting the transverse processes to each side of the vertebral body. The cartilage covered facets, two superior and two inferior on each vertebra, are the sites of articulation between adjacent vertebrae.

There are minor differences between the vertebrae of the different spinal regions. It is relevant to note that the thoracic vertebrae have demi-facets on each side of the vertebral body and full facets on each transverse process. These cartilaginous facets, which are also illustrated in Figure 2, serve as articulation sites for the ribs.

1.1.3 ANATOMY OF THE INTERVERTEBRAL DISCS

The intervertebral discs, shown in Figure 3, are composed of three structural components: the nucleus pulposus, the annulus fibrosus, and the cartilaginous end-plates. The nucleus pulposus is the gelatinous core of the disc. It has a high water content (70 - 90%) and contains a loose network of fibres. This nucleus comprises 30 to 50% of the entire disc structure. Surrounding the nucleus is a set of concentric rings of fibres known collectively as the annulus fibrosus. All the fibres in each band run in approximately the same direction and are oriented at 30 degrees to the horizontal plane of the disc. However, the fibres in adjacent rings run in opposite directions to create a separation of 120 degrees between bands. Near the nucleus pulposus, the annulus fibrosus is attached to the cartilaginous end-plates, and at the outer boundary, the annulus fibrosus is attached directly to the vertebral body. The cartilaginous end-plates are hyaline cartilage structures located between the fibrous components of the disc and the vertebral bodies.

1.1.4 LIGAMENTS OF THE VERTEBRAL COLUMN

There are six sets of spinal ligaments which act in unison to protect the spinal column from adverse loading conditions while still allowing sufficient physiological motion and flexibility. As shown in Figure 4, these are the anterior and posterior longitudinal ligaments, the ligamentum flavum, the articular capsule ligaments, the intraspinous ligament, and the supraspinous ligament. The anterior longitudinal ligament is a continuous fibrous band running from the first cervival vertebra (C1) to the sacrum which attaches to the anterior surfaces of the vertebrae. Similarly, the posterior longitudinal ligament attaches to the posterior surfaces of the vertebral bodies from C1 to the sacrum. The ligamentum flavum connects the lamina of adjacent vertebrae throughout the entire vertebral column. The articular capsule ligaments extend perpendicularly from the facets of each vertebra to connect to the facets of the adjacent vertebrae. Finally, both the intraspinous and the supraspinous ligaments connect the spinous processes of adjacent vertebrae.

1.1.5 ANATOMY OF THE RIB CAGE

The ribs, the sternum, and the spine are the main structures forming the osseocartilaginous cage known as the thorax or the rib cage. The elongated bone located at the middle front of the thorax is the sternum. The sternum, which consists of cortical bone surrounding a cancellous bone interior, provides attachment sites for the costal cartilage of the first seven ribs. The ribs are cylindrical bands of bone which extend from the vertebrae through the costal cartilages to the sternum. The ribs, which have elliptical cross-sections, are composed of cancellous bone in a cortical bone covering. There are twelve pairs of ribs: the first seven are true ribs that attach to the sternum, and the remaining five are false ribs. The false ribs either attach to the costal cartilage of the rib above (ribs 8,9, and 10) or end

freely in the chest cavity (ribs 11 and 12). Rather than projecting horizontally toward the sternum, the ribs are positioned at an oblique angle that increases from rib one to rib nine. The length of the ribs also increases from rib one to rib seven.

The spaces in between the ribs, the intercostal spaces, are lined with soft tissues known as the intercostal fascia or membranes. These membranes extend from rib to rib in an attempt to restrain the separation of adjacent ribs. The fascia are positioned at both 45 degrees and 135 degrees with respect to the midline of the ribs.

There are several defining features of the ribs, as shown in Figure 6. The rib head, neck, and tubercle are located at the vertebral end. The head is divided into two facets which connect to the bodies of the two adjacent thoracic vertebrae to form the costo-vertebral articulation. The rib neck serves as the attachment site for the costo-transverse ligaments. The tubercle of the rib contains an articular facet for attachment to the transverse process of the inferior thoracic vertebra. This junction is the costo-transverse articulation. The body of the rib extends from the tubercle and ends in a oval depression into which fits the end of the costal cartilage. This hyaline cartilage structure serves to elongate the rib and to articulate with the sternum at the costo-sternal junction. The maximum curvature of the rib occurs in the dorsal region known as the angle.

1.2 COORDINATE SYSTEM

The global coordinate system used in the model is shown in Figure 7. It is defined as follows:

-the positive x direction runs from the posterior (the back or dorsal portion) to the anterior (the front or ventral portion) of the vertebrae

-the positive y direction is medial (towards the midline of the body) to lateral (away from the midline of the body)

-the positive z direction is inferior to superior (vertically upwards).

The three planes associated with the body are as follows:

-the sagittal plane is the XZ plane

-the horizontal plane is the XY plane

-the frontal plane is the YZ plane.

The origin of this global coordinate system is located at the centre front node of the middle vertebra (T6).

1.3 SCOLIOSIS

1.3.1 ANATOMY OF SCOLIOSIS

There are several curves associated with the vertebral column. Kyphosis is defined as a spinal curvature which is convex posteriorly, and lordosis is defined as a spinal curvature which is convex anteriorly. In the normal spine, both a cervical and lumbar lordosis, as well as a thoracic kyphosis, exist. Scoliosis is defined as an abnormal lateral curvature of the spine with vertebral rotation. The thoracic spine is the most common location for scoliotic curves.

The scoliosis condition involves several physical characteristics: uneven shoulders and a crease in the waist due to the lateral curve, and a rib hump deformity associated mainly with the vertebral rotation [24]. Not only are there global abnormalities present with scoliosis

(lateral curve and vertebral rotation), but local abnormalities are also present. These deformities at the vertebral level include: asymmetry of the transverse processes, unequal pedicle lengths and widths, curvature of the spinous processes away from the midline, and vertebral body asymmetry.

1.3.2 TREATMENT OF SCOLIOSIS

Treatment of scoliosis involves eliminating or reducing both the lateral curve and the vertebral rotation in order to return the spine to as normal an alignment as possible . The most common, non-intrusive, method of treatment is bracing. The three most common braces used today are the Milwaukee Brace, the Boston Brace, and the Charleston brace [4]. This non-operative management of scoliosis uses a three-point system of applied forces to eliminate the spinal curve and to derotate the vertebrae [4]. A pressure pad is placed in the brace to apply a force on the apex of the curve. Two additional pads are placed on the opposite side of the brace to provide counter forces on the spine. However, since the thoracic spine is surrounded by the rib cage, these forces are not able to act directly on the vertebral column [4]. Instead the pads are placed over the ribs, and the forces are transmitted to the appropriate vertebrae through the costo-transverse and costo-vertebral articulations.

1.4 ANATOMY AND BIOMECHANICS OF THE ARTICULATIONS

1.4.1 COSTO-VERTEBRAL ARTICULATION

The costo-vertebral and costo-transverse articulations are mechanically linked. The simultaneous movement of these joints is a rotation about an axis passing through the centre of each articulation, as shown in Figure 8. For the lower ribs, the axis of rotation is

approximately parallel to the x-axis, and therefore the rib rotations cause an increase in the medial-lateral diameter of the rib cage. In contrast, the axis of rotation for the upper ribs is approximately parallel to the y-axis, and therefore an increase in the anterior-posterior diameter of the rib cage results from rib rotations.

The costo-vertebral articulation is limited to slight gliding motions by the mechanical function of three groups of ligaments [11]. These ligaments, which are shown in Figure 9, are:

1. The Articular Capsule: this strong group of ligaments surrounds the joint and connects the head of the rib with the circumference of the articular facet on the vertebral body.

2. The Radiate Ligaments: these ligaments extend from the anterior part of the rib head to the sides of the vertebrae and intervertebral discs.

3. The Intraarticular Ligament: this ligament located at the interior of the joint connects the middle of the rib head to the intervertebral disc.

1.4.2 COSTO-TRANSVERSE ARTICULATION

This gliding joint is governed by four sets of ligaments [11]:

1. The Articular Capsule: this capsule surrounds the articular surfaces on both the rib tubercle and the transverse processes,

2. The Interosseous Costo-transverse Ligament: this short and strong ligament connects the dorsal surface of the rib neck to the base of the inferior transverse process.

3. The Posterior Costo-transverse Ligament: this rectangular ligament extends from the lateral end of the tubercle to the apex of the inferior transverse process.

4. The Superior Costo-transverse Ligament: this thick, strong ligament runs from the superior surface of the rib neck to the lower surface of the superior transverse process.

The locations of these ligaments are illustrated in Figure 10.

1.4.3 THE COSTO-STERNAL ARTICULATION

Two sets of ligaments, the articular capsule and the radiate ligaments, blend together to control the movement of this joint. The articular capsule surrounds the joint and the radiate ligaments attach the sternal ends of the costal cartilage to the anterior and posterior surfaces of the the sternum. No rotation is permitted at this articulation, and only slight vertical translations are allowed.

1.5 MECHANICAL BEHAVIOUR OF BIOLOGICAL TISSUES

1.5.1 COLLAGEN

Collagen is the basic building material for almost all biological tissues. It is a protein consisting of long helical molecules. Several of these molecules group together to form fibrils, which in turn group together to form fibres, which, finally, group together to form tissues. Collagen is a viscoelastic structure which exhibits the following mechanical behaviours: stress relaxation, creep, and hysteresis [9].

1.5.2 LIGAMENTS

Ligaments are made from collagen fibres interspersed with cells and water. In order to obtain maximum efficiency in transmitting tension, the collagen fibres in ligaments are arranged in a parallel configuration. Although ligaments have good tensile strength, they are unable to carry any compressive loads. Ligaments in the body are also in a state of prestrain (i.e.. if a ligament were cut in the body it would "spring back" to a state of zero stress). Initially, ligaments will deform exponentially with increased loading before exhibiting linear load-deformation characteristics. Typical ligament movements occurring in the body are governed by this linear load-deformation relationship [9].

For the purposes of this project, the inability of ligaments to resist compressive loading was observed, and their load-deformation curves were assumed to be linear.

1.6 BIOMECHANICS OF THE SPINE AND RIB CAGE

1.6.1 THE RIBS

The ribs are flexible structures that are able to deform under loading. Displacements due to shear and axial loading of the ribs are negligible. However, three bending stiffnesses contribute to mechanical behaviour of the ribs, namely, resistance to bending in the superior-inferior direction, resistance to bending in the anterior-posterior direction, and resistance to torsional loading [6].

1.6.2 COSTAL CARTILAGE

The costal cartilages are approximately 40 times more flexible than the bony parts of the ribs [24]. The lower ribs have more costal cartilage than the upper ribs and are therefore more flexible and undergo more movement under loading conditions.

1.6.3 INTERVERTEBRAL DISCS

During normal physiological movements, the intervertebral discs are subjected to axial, shear, and torsional forces as well as bending moments in flexion, extension, and lateral bending [24]. The loading of the intervertebral disc is a complex coupling of many physiological movements. Compressive stresses are always present in the discs due to postural loading of the trunk and normal physical activity. In fact, the majority of the compressive loads occurring in the spine are carried by the intervertebral discs [24].

The load-deformation curve for the intervertebral disc experiencing compressive loading is non-linear. At low loads, the disc is flexible and offers little resistance to the loading. However, under higher loading conditions, the disc stiffness increases to provide greater stability to the spine [24]. Although the nucleus pulposus can only resist compressive loading, the orientation of the bands of the annulus fibrosus allow for effective resistance of normal physiological motions. However, the disc is sensitive to adverse bending moments and torsional loads.

FIGURE 1: The Vertebral Column (Modified from Gray [11])

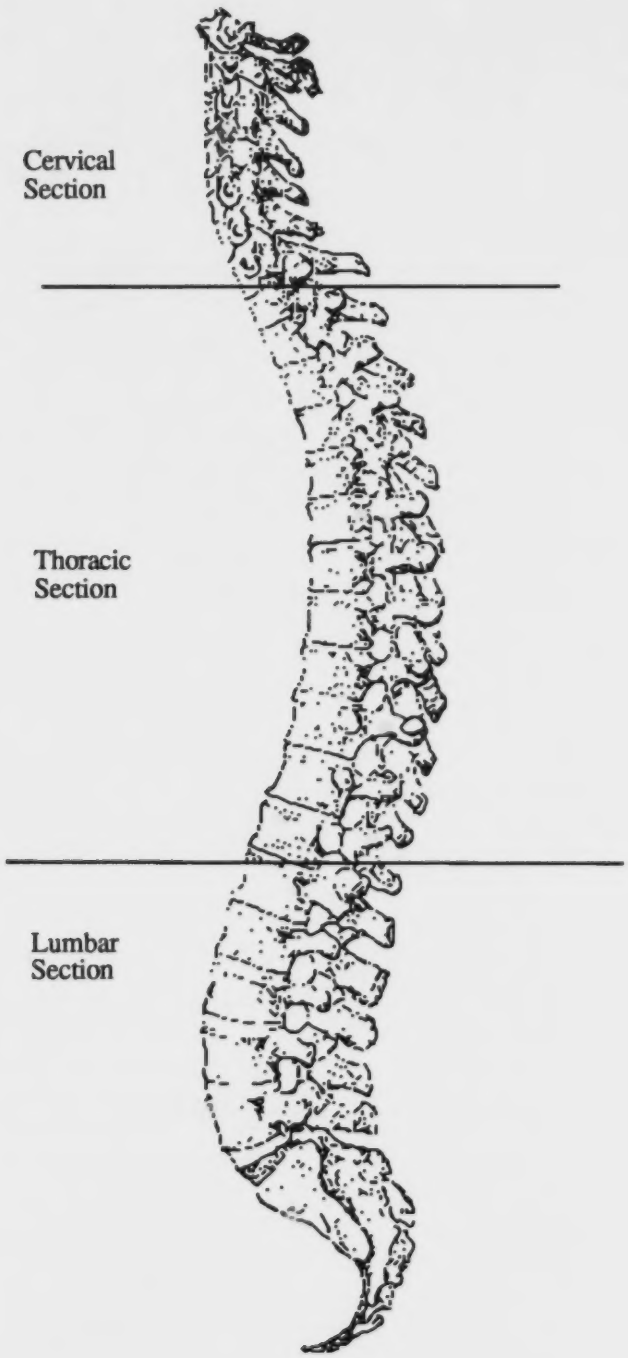

FIGURE 2: Components of the Vertebra (Modified from Gray [11])

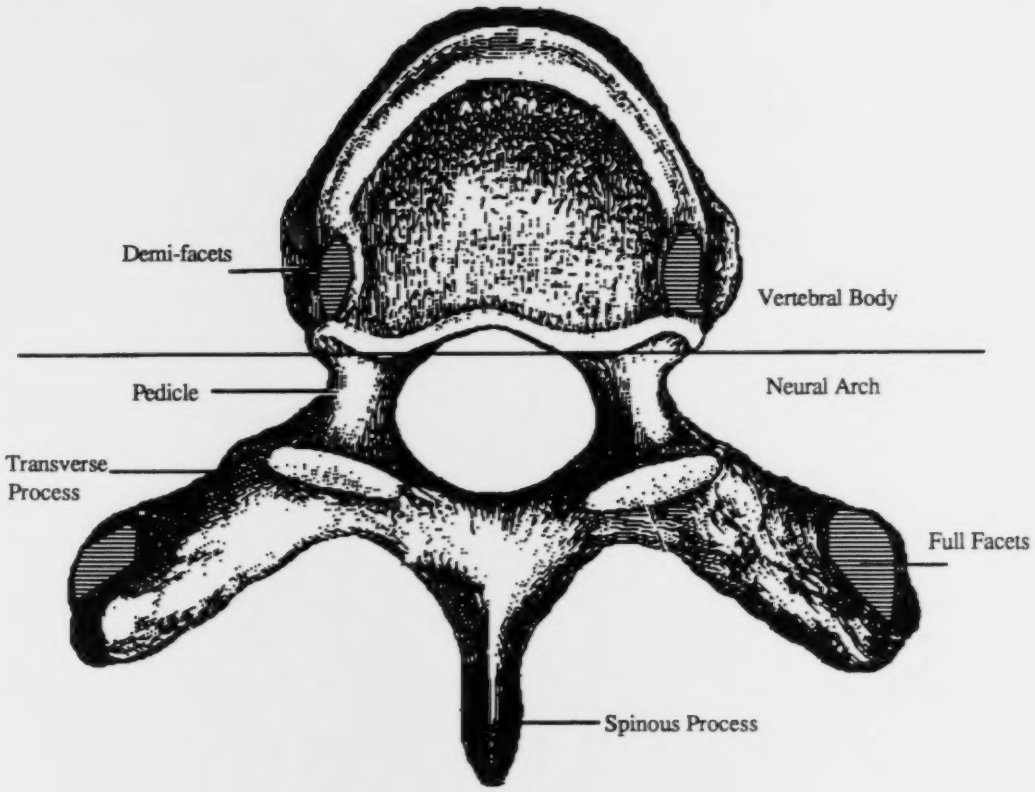

FIGURE 3: The Intervertebral Disc (Modified from White and Panjabi [24])

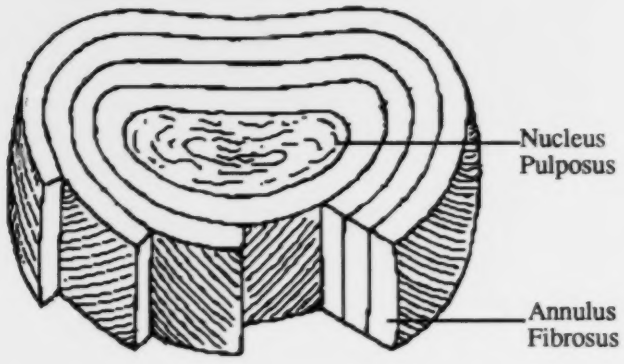

FIGURE 4: Ligaments of the Spinal Column (Modified from White and Panjabi [24])

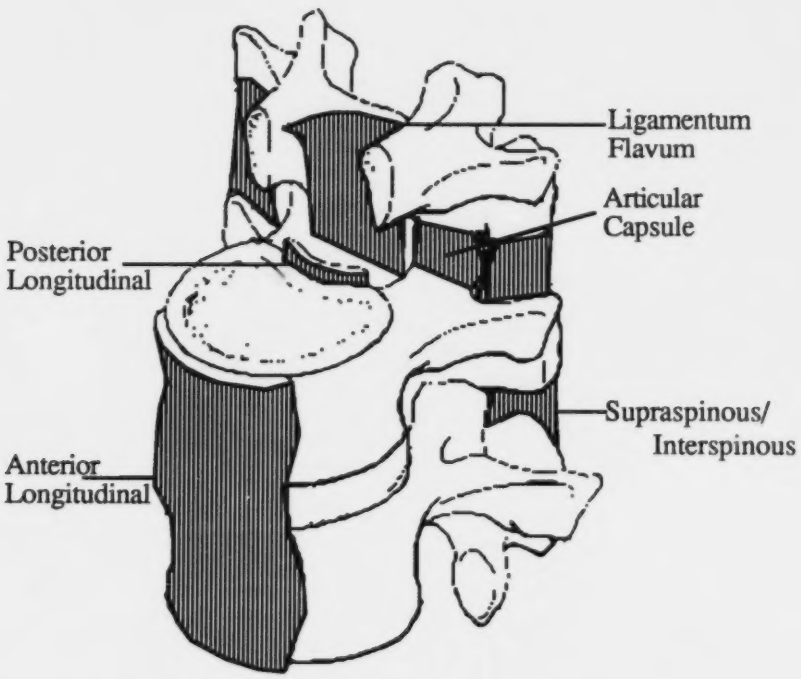

FIGURE 5: The Rib Cage (Dorsal View)
(Modified from Kapandji [12])

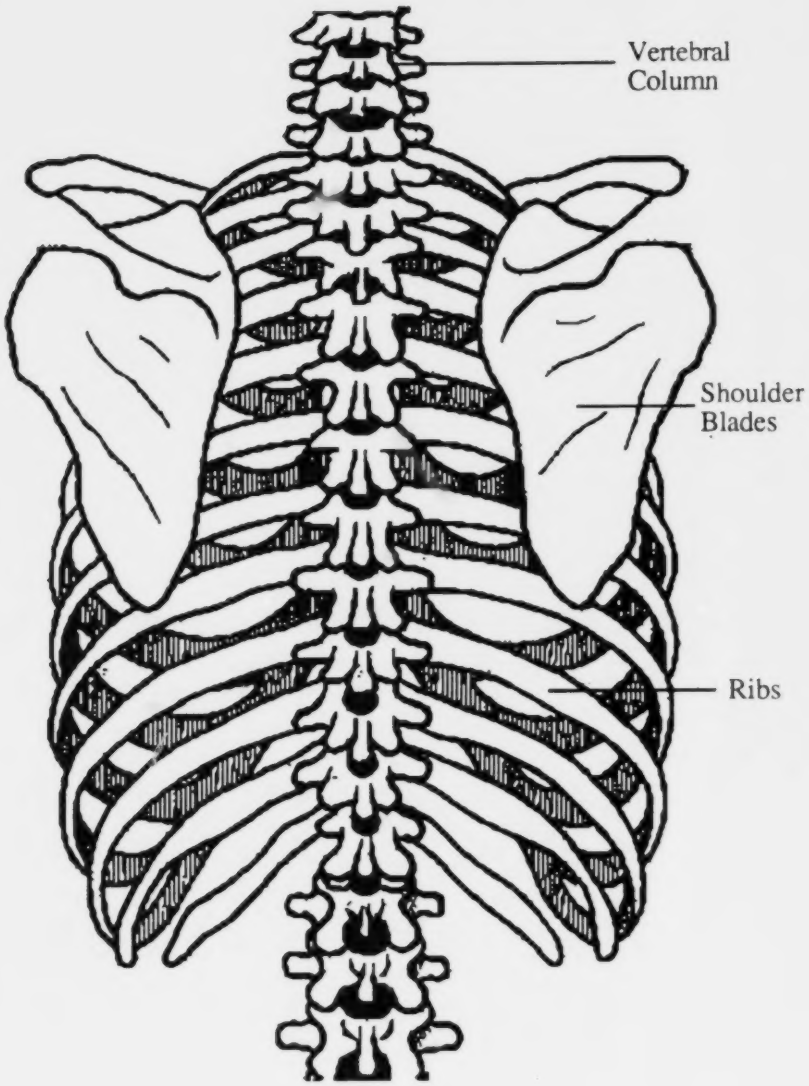

FIGURE 6: Components of the Rib (Modified from Gray [11])

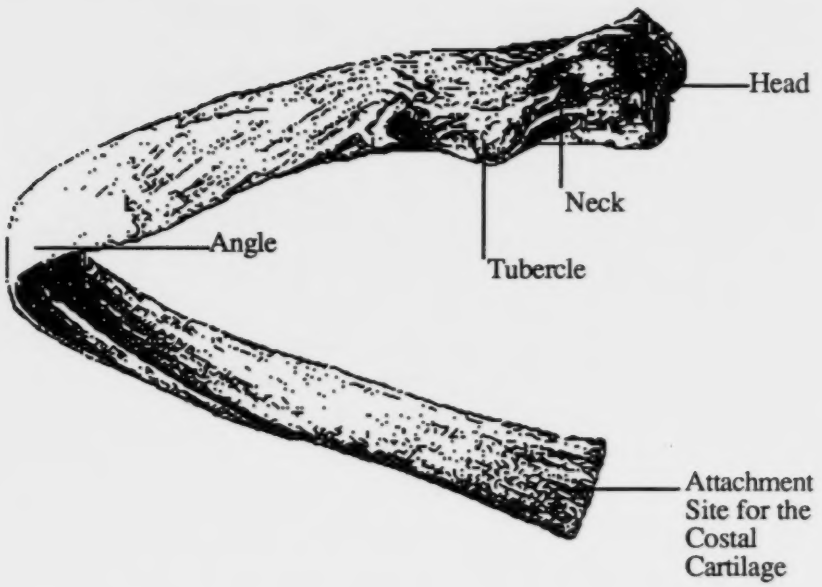

FIGURE 7: The Coordinate System (Modified from White & Panjabi [24])

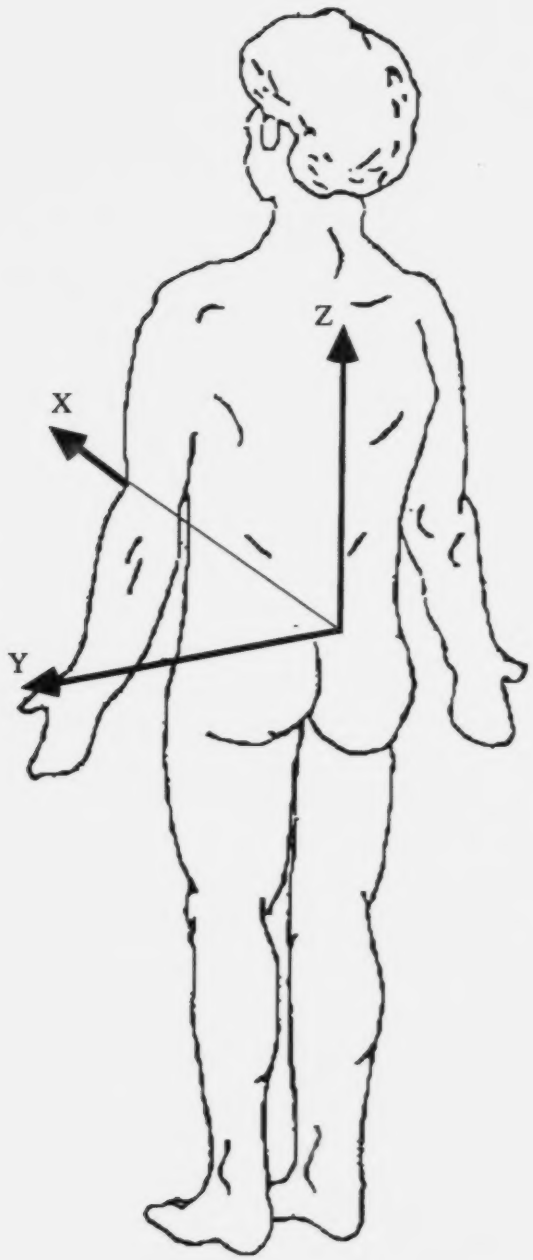

FIGURE 8: Movement of the Rib-Vertebra Articulation (Modified from Kapandji [12])
(The axis of rotation is shown)

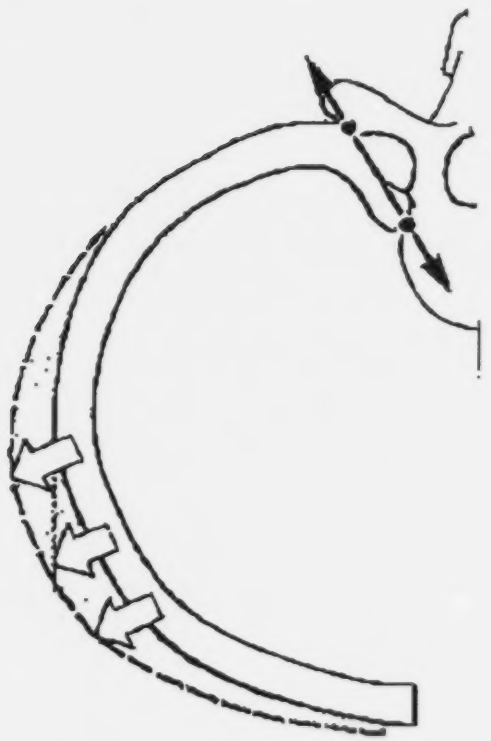

FIGURE 9: Ligaments of the Costo-Vertebral Articulation
(Modified from Kapandji [12])

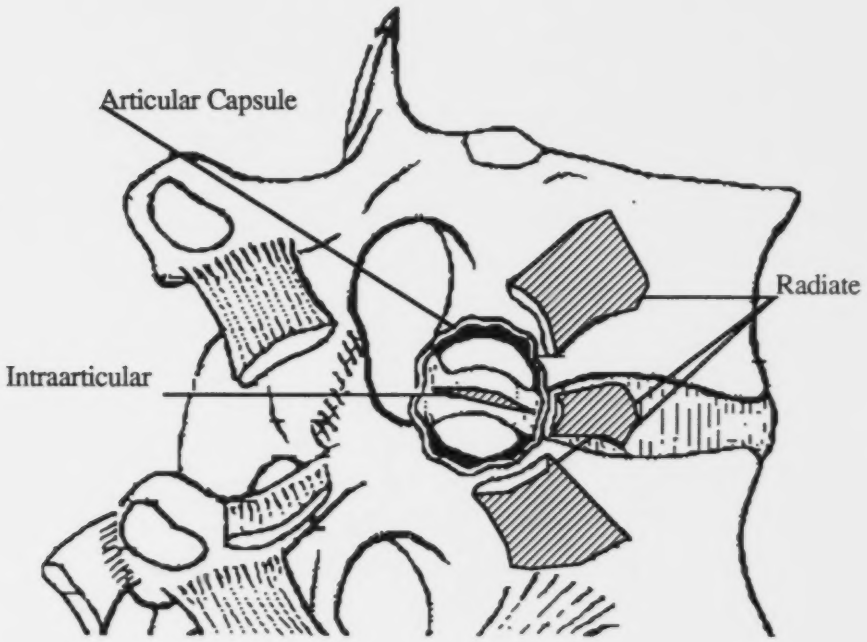

FIGURE 10: Ligaments of the Costo-Transverse Articulation
(Modified from Kapandji [12])

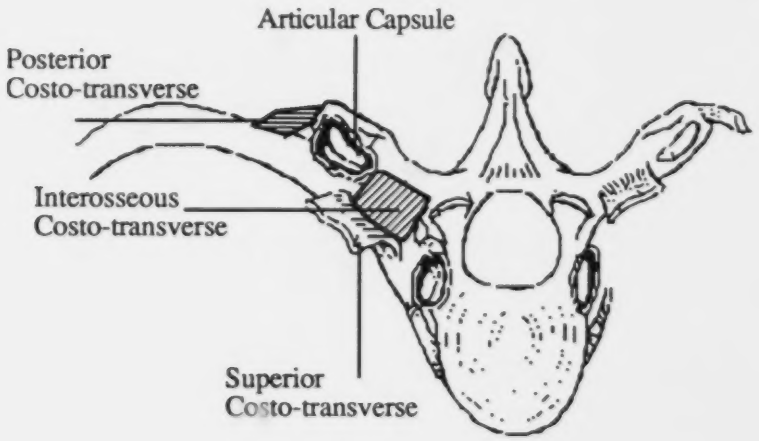

CHAPTER TWO: LITERATURE REVIEW

2.0 OVERVIEW OF THE LITERATURE REVIEW

Modelling of the human thorax was first performed in 1970 as a tool to investigate the kinematic response of the rib cage to impact. Since then, other finite element and mathematical models have been developed to study the effect of blunt trauma to the rib cage, as well as furthering the understanding of the mechanical behaviour of the thorax under both normal and pathological conditions. These models have also been used to investigate the probable causes and effects of scoliosis. Although each new model has attempted to improve upon the previous models, two overall limitations remain. First, difficulties have arisen with every model because of the lack of experimental data from which accurate material properties may be assigned. Second, an accurate model of the rib-vertebra articulation has not been developed. A variety of different approaches to modelling this area have been incorporated into the global models without meticulous validation of the simulated articulation. The Thompson model has incorporated many of the findings and recommendations of these studies, while attempting to overcome the second of these limitations. The boundary conditions and loading situations of these previously published models were not considered to be relevant in the development of the Thompson partial model of the rib cage.

2.1 ROBERTS AND CHEN [16]

Roberts and Chen developed a finite element model of the sternum, costal cartilage, the first ten ribs, and the vertebral column from T1 to the sacrum. 169 nodes were used to define the rib cage. Each of these nodes was connected by individual, rigid body members, and all elements were assumed to be rigidly connected. Physiological movements permitted at the costo-vertebral and costo-transverse articulations were not modelled.

Detailed data of rib cross-sectional properties are outlined in the paper. These properties were found using the following assumptions: the ribs have elliptical cross-sections and the effective area of the ribs (i.e.. the area of cortical bone) is 50% of the total rib area. All cortical bone and cartilage elements were assumed to be elastic, homogeneous, and isotropic.

The boundary conditions of the model simulated a person seated against a rigid back support. Movement at T1 was constrained in both the anterior-posterior (AP) and medial-lateral directions, and movement in ribs four through seven was constrained in the AP direction as well. No translations were allowed at the sacrum, and no external rotational constraints were imposed anywhere in the model.

Both concentrated and uniform line loads of 100lbs were applied at various locations on the sternum in the AP direction.

Using finite element techniques, displacements, forces, and stresses incurred in the model were calculated. Roberts and Chen concluded the following:

1. The assumption of a rigid connection at the rib-vertebra articulation is not valid. The flexibility of this joint must be modelled.
2. The costal cartilages will deform before failure and, therefore, need to be modelled with a sufficient number of elements to represent these displacements.
3. Rib bending stresses are highest in the angle of the rib.
4. The sternum moves as a rigid body.
5. The flexibility of the costo-sternal articulation must be modelled appropriately.

2.2 SCHULTZ, BELYTSCHKO, AND ANDRIACCHI [17]

This mathematical model represented the thoracolumbar spine complete with ligaments and intervertebral discs. The vertebrae were modelled as rigid bodies, and deformable elements were used to model the ligaments and discs. One set of these deformable elements, extending from adjacent centres of vertebral endplates, were assigned appropriate axial, bending (flexion, extension, and lateral bending), shear and torsional stiffnesses to accurately model the intervertebral discs. Ten springs per vertebra were used to model the ligaments connecting the posterior elements. To fully simulate the biomechanical behaviour of ligaments, which cannot resist compression, these springs were assigned tensile stiffnesses only. Finally, the four elements modelling the articular facets were assigned both tensile and compressive stiffnesses to model both the kinematic constraints of the bone-to-bone contact as well as the deformation-resistance properties of the facet ligaments.

The study focussed on a spinal motion segment consisting of two adjacent vertebrae and their connecting disc and soft tissues. The inferior vertebra was rigidly fixed while the

movements of the superior vertebra were unrestrained. Tensile, compressive, and shearing loads, as well as flexion, extension, and lateral bending moments were applied to the superior vertebra.

Using this spinal model, Schultz *et al* . concluded:

1. The ligaments and facet joints of the spine play an important role in resisting deformation due to applied loading.
2. The material properties of the different spinal levels may be extrapolated using known level-to-level geometrical changes.
3. The limiting factor in the accuracy of this model is the inadequate information available concerning geometrical and material properties of the spine.

2.3 ANDRIACCHI, SCHULTZ, BELYTSCHKO, AND GALANTE [3]

This mathematical model consists of rigid body elements representing the thoracolumbar spine, the bony sections of ribs one to ten, the sternum, and the sacrum. These elements are interconnected with deformable elements representing the intervertebral discs, the costal cartilages, the joint capsules, and the ligaments.

This model incorporated the earlier spine model developed by Schultz *et al.* To improve on the Roberts and Chen study, the costo-vertebral articulation was modelled using a bilinear spring which is ten times more stiff in compression than in tension. A beam element which is able to resist all bending moments and axial, shear, and torsional loads, was used to model the costo-transverse articulation. The costal cartilages were modelled using beam elements that exhibit axial, bending, and torsional stiffnesses. Spring elements were used to model the intercostal membranes.

Two boundary and loading conditions were applied to this model. The first constrained all motion at the sacrum while constraining T9 in the sagittal plane only. Using these boundary conditions, a load was applied along the lower five ribs to simulate a 100N lateral squeezing force. The second condition constrained all movement at both T1 and T9 in the sagittal plane while applying a compressive load in the AP direction to the sternum.

This model gave rise to the following conclusions:

1. The kinematics of the costo-vertebral and costo-transverse articulations play a significant role in the mechanical behaviour of the spine and rib cage.
2. Under the applied loading, deformations of the costal cartilages occurred.
3. Under the applied loading, the bony sections of the ribs experienced rigid body motion.
4. The rib cage enhances the ability of the isolated spine to resist deformation due to compressive loading and lateral bending.

2.4 CLOSKEY, SCHULTZ, AND LUCHIES [6]

This study extended the Andriacchi study by dividing the ribs into five cylindrical bodies connected by four beam elements. This allowed the bony part of the ribs to deform under loads. The beam elements were assigned three bending stiffnesses: 20 N-m/rad in AP bending, 18 N-m/rad in superior-inferior bending, and 30 N-m/rad for torsional loading. The authors concluded that by allowing deformation of the ribs, their model produced output which more closely simulated experimental results.

2.5 SUNDARAM AND FENG [23]

In Sundaram and Feng's finite element analysis of the thorax, they modelled the ribs, costal cartilage, the sternum, the vertebrae, the intervertebral discs, the muscles, and the gross heart and lung organs. The thoracolumbar spine was represented using 36 beam elements, the sternum was modelled using six quadrilateral plate elements, and the ribs were modelled as linear beam elements (four per rib). Beam elements were also used to represent the costal cartilages.

Sundaram and Feng also investigated the effects of cartilage in bending and concluded that its Young's Modulus is twenty times greater in compression than in tension. All materials were assumed to be linearly elastic.

The applied boundary conditions constrained all points in the sagittal plane of symmetry from lateral translations and from rotations about the vertical and AP axes. Selected points were also restrained from movement in the AP direction, and the sacrum was rigidly fixed.

Eleven different loading conditions were applied, all in the AP direction. The first ten loads were concentrated loads of 50lbs each applied at ten different nodes. The final loading condition was a pressure of 5 psi exerted on the sternum.

Sundaram and Feng concluded:

1. The sternum moves as a rigid body.
2. The bending stresses incurred in the ribs are larger than the axial stresses.

2.6 STOKES AND LAIBLE [22]

Stokes and Laible introduced a finite element, osseo-ligamentous structural model of the spine and rib cage. They modelled the ribs and the sternum using beam elements and the intercostal membranes with spring elements. The costo-vertebral articulations were modelled as ball and socket joints. The costo-transverse joints were modelled with flexible beam elements.

Stokes and Laible used two different boundary conditions for their model. The first allowed only flexion at the fifth lumbar vertebra (L5), and flexion and vertical translation at the first thoracic vertebra (T1). The second condition permitted all three rotations at L5 while constraining only horizontal translations at T1.

This model was used to apply asymmetric growth conditions in an attempt to initiate a scoliosis condition in the spine. The resulting model curves were smaller than actual physiological measurements. Stokes and Laible concluded that this discrepancy was due to a lack of axial rotation in their model .

2.7 MATERIAL PROPERTIES

Table 1 lists the different material properties for bone, cartilage, intervertebral discs, and ligaments that are published in the literature. Most of these studies list only the material properties. They make no mention of the testing methods used to arrive at these values. The only notable exception involves the ligament stiffness values. For this, most authors used previously published experimental results to determine these parameters [17]. This experiment by Schultz *et al.*, performed more than twenty years ago, involved hanging weights equivalent to a 7.5 Newton force from cadaveric ribs. The resulting displacements

were then measured. Six different cadavers were used and a large range of displacements were reported. Table 1 reflects this variation in these results since it is this data that was used to assign the stiffness values for the articulation ligaments.

TABLE 1: Material Properties and Stiffness Values from the Literature

Authors	Bone*	Cartilage*	Ligaments	IV Discs
Roberts & Chen	E=12 000 MPa v=0.2	E=275 MPa v=0.1		
Sundaram & Feng	E=12 000 MPa v=0.2	E=480 MPa v=0.1		E=10.3 MPa v=0.2
Stokes & Laible	E=12 000 MPa	E=480 MPa	Intercostals: E=5 MPa	
Schultz et al			k=5-25 N/mm	k=600-9000 N/mm
Andriacchi et al			k=5-125 N/mm k=2500-10 000 Nmm/rad	
Closkey	Ribs: k=10 000N/mm		k=50-1000N/mm k=3500-7500 Nmm/rad	k=180-1090 N/mm k=22 000-78 000 Nmm/rad

* indicates isotropic materials
E = Young's Modulus v = Poisson's Ratio k = stiffness

CHAPTER THREE: MODEL DESCRIPTION

3.0 PROPOSED MODEL

3.0.1 MODEL COMPONENTS

The Algor Finite Element Analysis System's linear stress analysis package for the IBM RISC 6000 was used to model a section of the spine and rib cage [2]. The model components are as follows:

-vertebrae T5, T6, and T7

-the intervertebral discs

-ribs 6 and 7

-the corresponding portion of the sternum

-the intercostal membranes

-all associated ligaments of the joints and vertebral column.

The spinal ligaments included in the model are the anterior and posterior longitudinal ligaments, the capsular ligaments of the articular facets, the ligamentum flavum, the intraspinous ligaments, and the supraspinous ligaments. The following ligaments associated with the rib articulations are also included in the model: the superior, posterior, and interosseous costo-transverse ligaments, and the radiate ligaments and articular capsule of the costo-vertebral articulations.

A model of a lumbar spinal motion segment had previously been constructed and validated [20]. This model was subsequently modified to represent the thoracic vertebrae T5, T6, and T7, complete with ligaments and intervertebral discs [21]. The present model builds on this work by adding in the remainder of the components to simulate a section of the human thorax.

Figures 11 through 14 are different views of the Thompson model. A side view of the model showing the locations of the boundary elements is found in Figure 11. The intervertebral discs, the ligaments, and the intercostal membranes have been omitted for clarity. Figure 12 shows only the ribs and the intercostal membranes. Note in this figure the diagonal pattern of the intercostal membranes. Additionally, the applied forces are shown with arrows. A plan view of the Thompson model (again without the intercostal membranes) is shown in Figure 13. Finally, Figure 14 shows an expanded view of the rib-vertebra articulation with particular emphasis on the articulation ligaments.

3.0.2 ELEMENT TYPES

Beam elements were used to model the ribs since actual ribs are able to resist bending and torsional moments as well as axial and shear forces. Ligaments, on the other hand, only exhibit axial stiffness properties. For this reason, truss elements were used to model ligament behaviour. Although the intervertebral discs resist forces and moments in all directions, only uniaxial truss elements were used in the disc model. A system of six sets of these trusses was designed to accurately represent the mechanical behaviour of the intervertebral discs. Finally, since only large, rigid body translations of the vertebrae and sternum were to be investigated, brick elements were used in the construction of these structures.

370 three-dimensional, 8-node brick elements are used to model the vertebrae and the sternum. 52 truss elements are used to model the intervertebral discs. 144 beam elements are used to model the ribs and costal cartilages, while 108 truss elements are used to model the intercostal membranes. A total of 100 truss elements are used to model both the spinal and articulation ligaments. 28 truss elements are also used to model the bone-to-bone contact which occurs at the costo-transverse joint, the costo-vertebral joint, and the facet joints of the vertebrae.

3.0.3 NON-LINEAR LIGAMENT BEHAVIOUR

As mentioned previously, ligaments are non-linear in that they cannot resist compression. To more fully simulate this behaviour while using linear truss elements, after each run or model simulation, all ligaments were checked and those that were found to be in compression were eliminated and the run was redone. Similarly, the bone-to-bone contact truss elements were also checked and those found to be in tension were eliminated.

3.1 GEOMETRIC DESCRIPTION

3.1.1 RIB DATA

The midline of each rib was modelled using 18 linear beam elements. Results from experimental work [18] were used to assign cross-sectional properties to each beam element. These properties (area and moments of inertia) were interpolated from the graphs of the published data for ribs six and seven [16]. The effective cross-sectional areas, i.e. the area of cortical bone in the ribs, ranged from 36.7 mm^2 to 79.5 mm^2. In the absence of any right to left variations in rib properties, cross-sectional properties were assigned to 38 different locations in the ribs and costal cartilages. In the human body, the ligaments of the

rib-vertebra articulations attach to the outer surfaces of the ribs rather than to the rib midlines. For this reason, an additional 16 linear beam elements were used per rib-vertebra articulation to account for the offset. These bony protrusions, which serve as attachment sites for the articulation ligaments, are shown in Figure 12.

In 1974, Schultz *et al.* published measurements of rib geometry [18]. The mean values of this data for rib six, and interpolated values for rib 7, were used to construct the present model. The parameters published by Schultz *et al.* include: the perpendicular distance between rib ends, the angle of the approximately circular arc of the rib, the x and y coordinates of one endpoint and the centre of this arc, and the perimeter of the rib.

The angles formed by the ribs in both the frontal and lateral planes were obtained from Dansereau [7]. These angles are 10.4 degrees and 37.2 degrees respectively for rib six and 10.9 degrees and 39.0 degrees for rib seven.

3.1.2 ARTICULATION GEOMETRY

A companion study by Schultz, to the one outlined above, includes measurements of the costo-vertebral and costo-transverse articulations [19]. This data described the posterior distances of both the costo-vertebral and costo-transverse articulations from the anterior edge of the vertebral body, as well as the lateral distance of the costo-transverse articulation from the centreline of the vertebral body. Anatomy textbooks [11, 12] were also used to determine the correct anatomical positioning of the associated ligaments.

Figure 15 shows an isometric view of the rib head and the ligaments of the rib-vertebra articulation. The associated vertebrae were omitted for clarity. Originally only one ligament was used per articular capsule. However, this resulted in rigid body rotations of

the rib head about the rib midline. To eliminate these undesirable moments, each articular capsule is now modelled using four truss elements.

Since the only physiological movements permitted at the costo-sternal articulation are very small, vertical, gliding motions, the costal cartilages of the ribs were assumed to be rigidly connected to the sternum.

3.1.3 STERNUM AND VERTEBRAE

The position and orientation of the sternum used in the model were determined from Gray's anatomy [11] and from a physical reconstruction of the human thorax.

The dimensions of the model vertebrae were determined from morphological studies reported by Panjabi and Dumas [8, 13]. The Panjabi study included measurements of the posterior vertebral body height, the upper and lower endplate widths and depths, the upper and lower endplate inclinations from the transverse plane, the pedicle width and height, the pedicle inclination from the transverse plane, the angle between the pedicle and the sagittal plane, the distance from the centre of the upper endplate to the tip of the spinous process, the span of the transverse processes, the articular facet area, and the angle between the articular facets and the frontal plane. The Dumas study concentrated on the orientation of the articular facets of the vertebrae.

3.2 MATERIAL PROPERTIES

3.2.1 CORTICAL BONE

The vertebrae, the sternum, and the truss elements representing bone-to-bone contact are all formed from cortical bone. These were assigned a Young's Modulus of 12 000 MPa and a Poisson's Ratio of 0.3 to correspond to the properties used in the original spine model [20].

3.2.2 RIB MATERIAL PROPERTIES

The bony sections of the ribs, which were assigned the cross-sectional properties published by Roberts and Chen, were originally given a Young's Modulus of 12 000 MPa and a Poisson's Ratio of 0.3 [16]. The model ribs were then compared to experimental work published by Schultz *et al* [18]. This study involved embedding the vertebral end of the rib in bone cement and applying a +/- 7.5 Newton load (in all three directions) at the sternal end. This fixed-free testing procedure was simulated with rib six of the model. Schultz reported rib movements ranging approximately from 1 to 30 mm depending on the direction of loading. Once the Young's Modulus for the bony sections of the ribs in the model had been adjusted to 20 000 MPa, movements of the sternal end of rib six ranged from 12 to 20 mm. Figure 16 is a graph depicting the comparison of the model rib displacements to the published experimental results.

3.2.3 SPINAL LIGAMENTS

Several stress-strain studies were used to assign stiffness values to the spinal ligaments used in the original thoracic spine model [5, 10]. Table 2 lists these stiffness values. To obtain these values, trial material properties were assigned to the spinal ligaments. An iterative approach then followed whereby the stress-strain curves of the model ligaments were compared to the results of two published studies. The stiffness values were assumed to be accurate when the model output was within the range specified by the experimental data. Figure 17 is a comparison of these stress-strain relationships. Only the graph for the supraspinous ligament is shown since its mechanical behaviour is considered to be representative of the behaviour of all the spinal ligaments. As evidenced by this figure, the mechanical properties of the spinal ligaments in the model are within the range suggested by previous studies.

TABLE 2: Material Properties of the Spinal Ligament Elements

Ligament	E(MPa)	A(mm^2)
Anterior Longitudinal	20	30
Posterior Longitudinal	20	20
Articular Capsule	25	21
Ligamentum Flavum	20	24
Interspinous	10	14
Supraspinous	10	10

3.2.4 COSTO-TRANSVERSE AND COSTO-VERTEBRAL ARTICULATIONS

The force-deformation properties of fresh, cadaveric rib-vertebra (costo-transverse and costo-vertebral articulations) junctions were investigated and reported by Schultz *et al.* [19]. Five rib-vertebra junctions (for rib 6) were tested in the following manner: the corresponding vertebra was secured in the testing fixture, and loads of 7.5 Newtons were applied to the rib just lateral of the costo-transverse articulation. The loads were applied in the superior, inferior, anterior, posterior, and lateral directions. The present model was used to simulate this experiment using the right side rib-vertebra articulation of rib six. The results of this procedure were used to assign stiffness values to the various ligaments of the costo-vertebral and costo-transverse articulations.

Although five specimens were tested, the paper only shows results for two of the specimens under lateral loading. Only two displacement values were obtained, and these were less than 2 mm; the absence of the other three measurements may be explained by the authors' expression of difficulty in obtaining accurate measurements of the small displacements incurred in the junction.

Schultz reported rib displacements ranging from 1mm to 11mm for the different loading conditions. Table 3 provides a summary of the ligament stiffnesses which were required to produce displacements ranging from 0.4mm (under lateral loading) to 5.7 mm (under superior loading). Figure 18 provides a graphical comparison of the Schultz experimental displacements and the present model simulation displacements. As can be seen from this figure, the assigned stiffness values produce displacements similar to the experimental output.

TABLE 3: Stiffness Values for the Ligaments of the Rib-Vertebra Articulations

LIGAMENT:	Articular Capsule	Radiate	Superior Costo-transverse	Costo-transverse
STIFFNESS: (N/mm)	58.29	19.67	6.75	8.33

3.2.5 COSTAL CARTILAGE

The Schultz study also investigated the force-deformation properties of fresh, cadaveric costo-sternal articulations [19]. This paper was used to adjust the properties of the costal cartilage beam elements in the model until model displacements most accurately duplicated experimental output. Loads of 7.5 Newtons were applied in the superior, inferior, anterior, and posterior directions approximately 1 cm medial of the lateral end of each costal cartilage. Schultz *et al.* reported displacements ranging from 5 mm to 11 mm occurring at the point of loading.

The costal cartilage beam elements were assigned a Young's Modulus of 275 MPa and a Poisson's Ratio of 0.1 [16]. The cross-sectional moments of inertia were modified from the Roberts and Chen values of $I_y = 811.8\ mm^4$ and $I_z = 153.4\ mm^4$ to $I_y = 1200\ mm^4$ and $I_z = 285\ mm^4$. This resulted in an improvement of output displacements from a range of 7.7 mm to 18.1 mm to a range of 7.3 mm to 11.1 mm.

Table 4 lists the final stiffnesses for the costal cartilage beam elements used in the model, and Figure 19 shows the resulting comparison between model and experimental results.

TABLE 4: Stiffness Values for the Costal Cartilage Elements

Axial (N/mm)	Shear (N/mm)	Flexion-Extension (N-mm/rad)	Lateral Bending (N-mm/rad)	Torsional (N-mm/rad)
1079	791	18 333	77 193	3836

3.2.6 INTERCOSTAL MEMBRANES

The material and sectional properties for the intercostal membranes were found from published data [22]. These truss elements were given a Young's Modulus of 5 MPa and a cross-sectional area of 20 mm^2.

3.2.7 INTERVERTEBRAL DISCS

In the lumbar spine model, described in Section 3.0.1, a detailed representation of the intervertebral disc was constructed from three-dimensional, 8-node brick elements. This brick disc was then scaled in the x, y, and z directions to match the gross thoracic dimensions reported by Panjabi [13]. The stiffness parameters of this disc model were found to be within the range of published data [6, 13].

A system of trusses was developed to replace the computationally intense brick model. Six groups of trusses are used to represent the six stiffness parameters of the disc: axial tension and compression, lateral and AP shear, flexion and extension, and lateral bending. Each group of trusses interferes only minimally with the action of the other groups. Thus, it is possible to calibrate the different stiffness parameters of the disc separately. Table 5 summarises the stiffness values used in the model and compares them to previously published data.

TABLE 5: Intervertebral Disc Stiffness Parameters

Model	Axial (N/mm)	Shear (N/mm)	Torsional (Nmm/rad)	Lateral Bending/Flexion/Extension (Nmm/rad)
Closkey	993	195	78 000	51 000 - 68 000
Panjabi	780	105	153 000	148 000 - 153 000
Thompson	780	100	150 000	130 000

3.3 APPLIED LOADING

A previous study was undertaken to determine the magnitude and direction of pressures applied by a Charleston brace on the trunk of a child [15]. The magnitudes were obtained from circular pressure transducers (20 mm diameters) mounted in the brace during use by the child, and the directions were obtained from x-rays showing the locations of the pressure transducers. Using these results, a force of 0.17 Newtons in the anterior direction and a force of 2.48 Newtons in the medial direction were applied at approximately one third of the way along the rib midline from the vertebral end. This loading condition is shown in Figure 12. This load was distributed evenly over both rib six and rib seven.

3.4 BOUNDARY CONDITIONS

The model contains not only the intervertebral discs between each of T5, T6, and T7 but also the intervertebral discs connecting T4 to T5 and T7 to T8. The truss elements representing these boundary discs are constrained from translations in all three directions at the ends not connected to T5 and T7. This simulates a situation in which the T4 and T8 vertebrae are rigidly fixed (i.e. restrained from motions in all three directions).

The ribs are constrained using truss elements representing the intercostal membranes adjacent to the superior border of rib six and the inferior border of rib seven. The original

lengths of these truss elements were equal to the physiological distance between rib five and rib six. This configuration is shown in Figure 20. These elements were then extended until any axial forces that occurred under loading were less than 1 Newton. This results in a situation in which all ribs respond to applied loading instead of the situation where only ribs six and seven move in isolation. Figure 21 illustrates this extension.

The superior and inferior borders of the sternum are constrained from translation in all three directions.

FIGURE 11: Side View of the Model
(Circles indicate the Boundary Conditions)
(Intercostal Membranes, Ligaments, and Intervertebral Discs Not Shown)

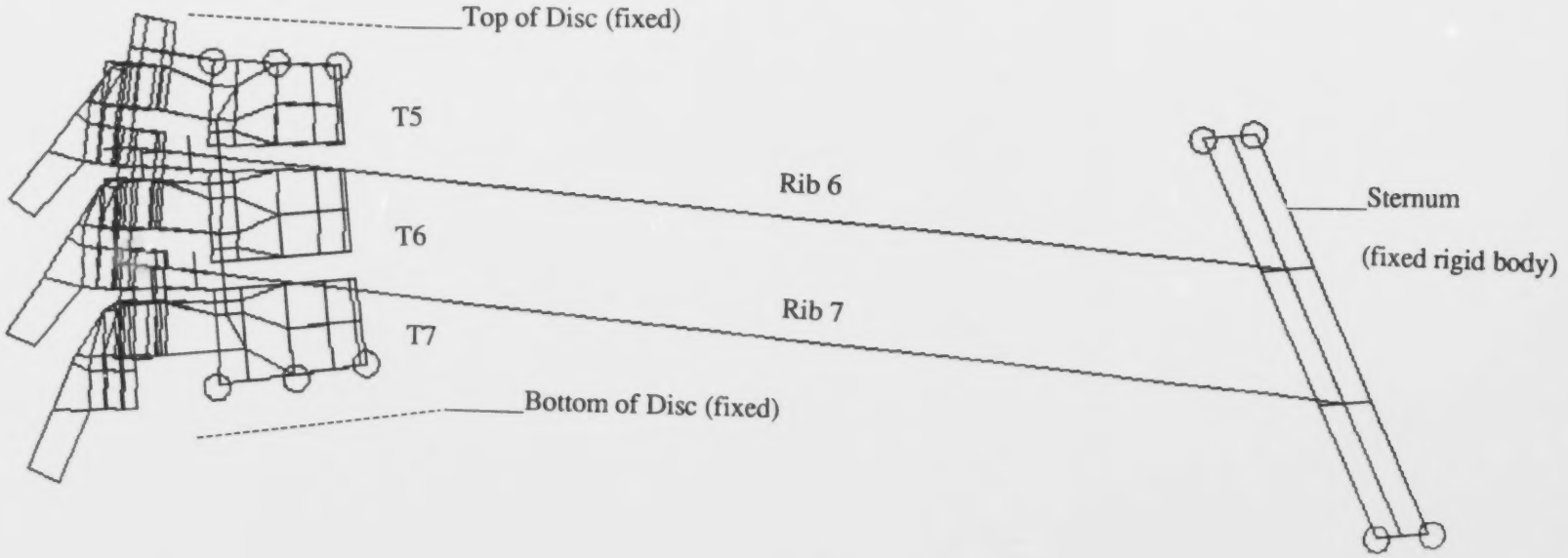

FIGURE 12: Isometric View of the Model Ribs and Intercostal Membranes
(Arrows indicate the Loading Condition)

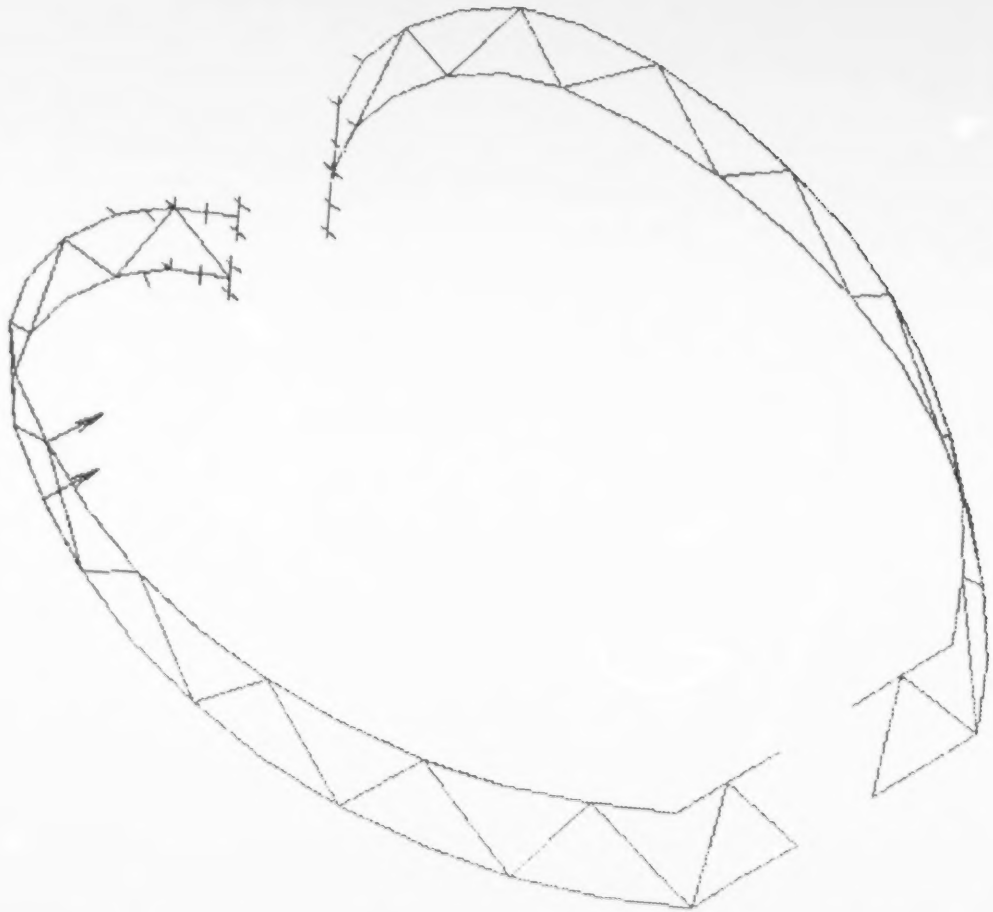

FIGURE 13: Plan View of the Model (without Intercostal Membranes)

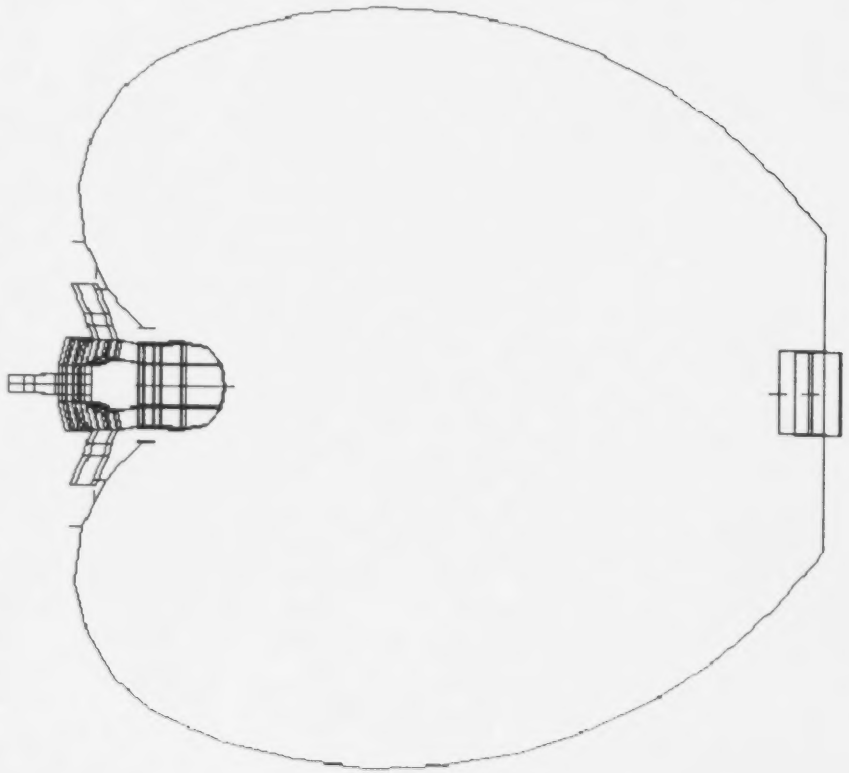

FIGURE 14: Diagram of the Rib-Vertebra Articulation

LIGAMENTS

A -- Posterior
Costo-transverse

B -- Interosseous
Costo-transverse

C -- Superior
Costo-transverse

D, E --Radiate

* -- Location of
Centre of Articular
Capsule

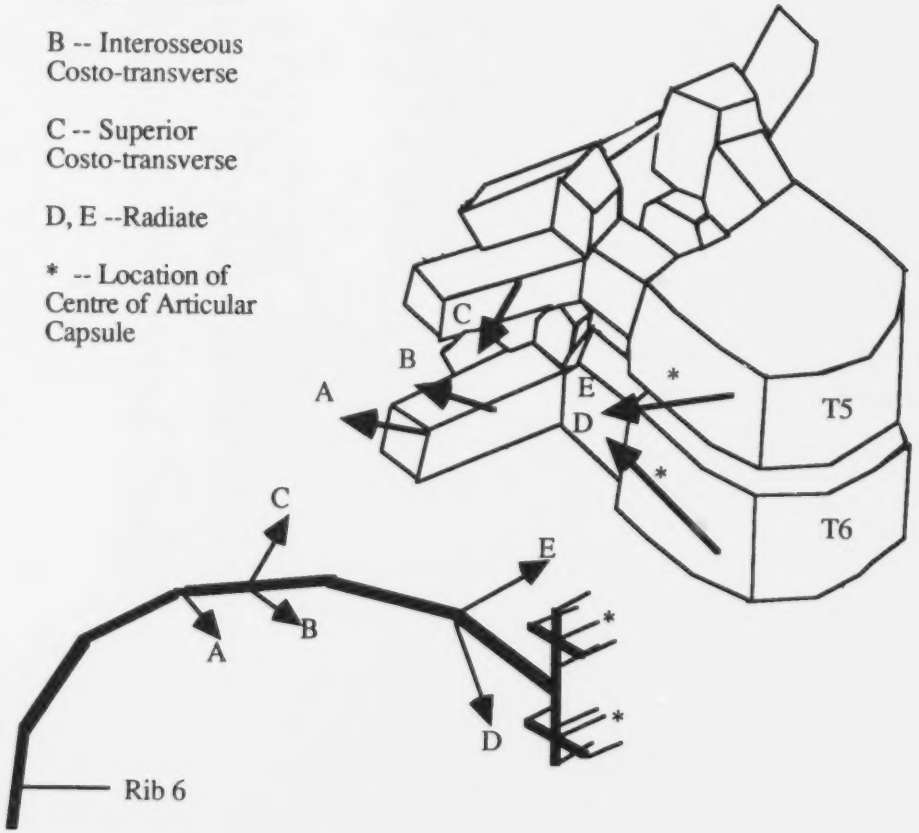

FIGURE 15: An Isometric View of the Ligaments of the Rib-Vertebra Articulation

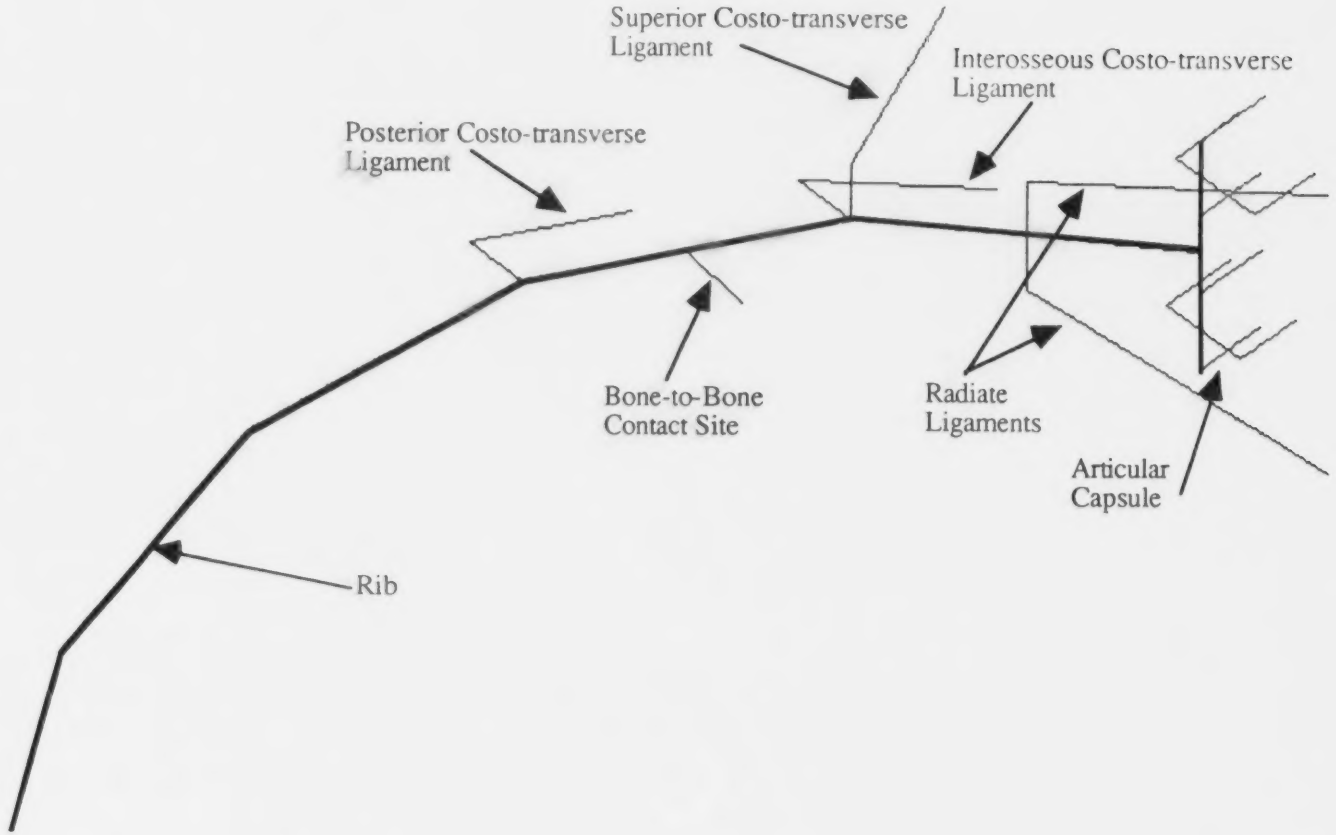

FIGURE 16: Validation of Rib Elements

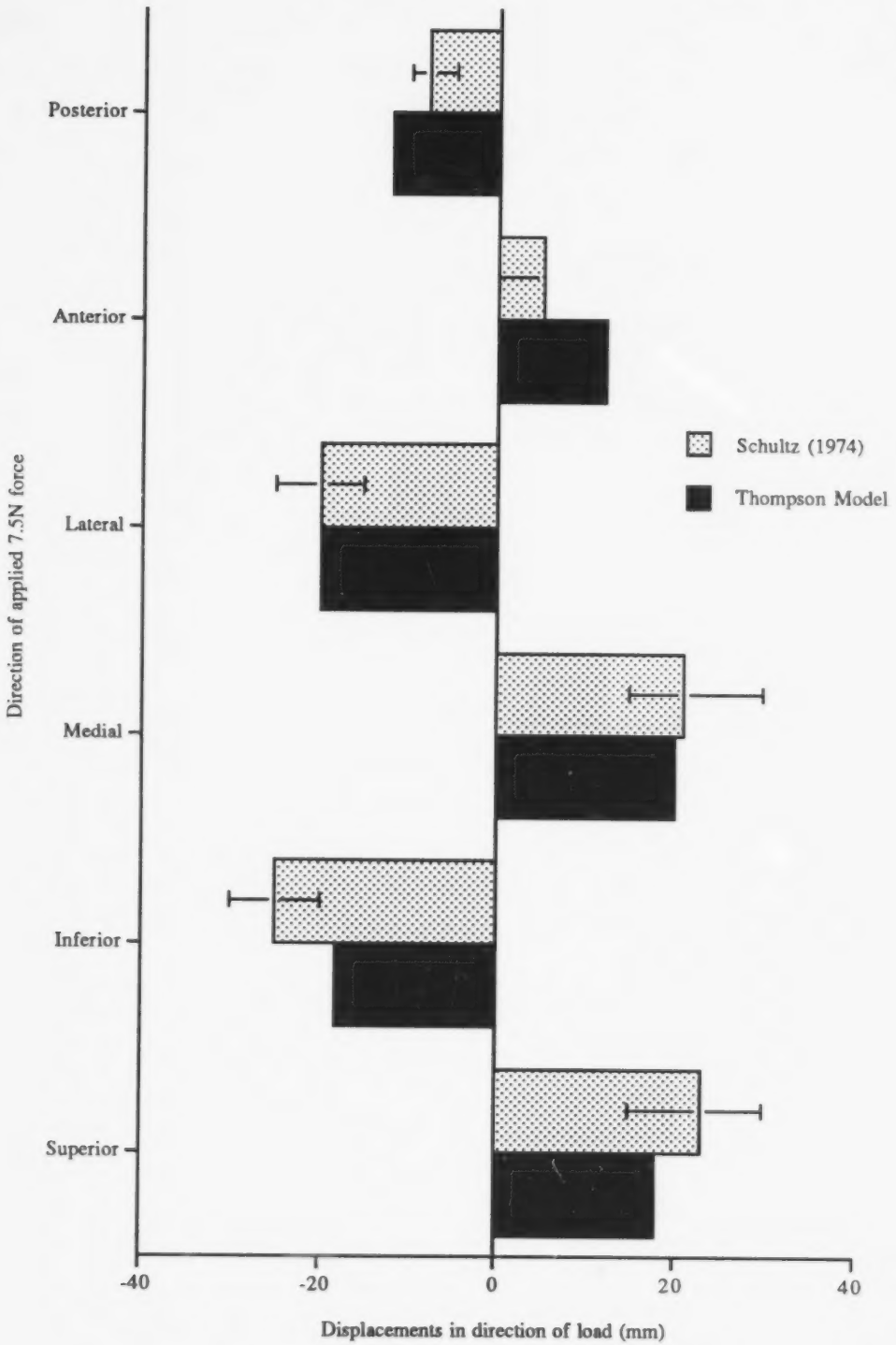

FIGURE 17: Stress Strain Relationship for Spinal Ligaments

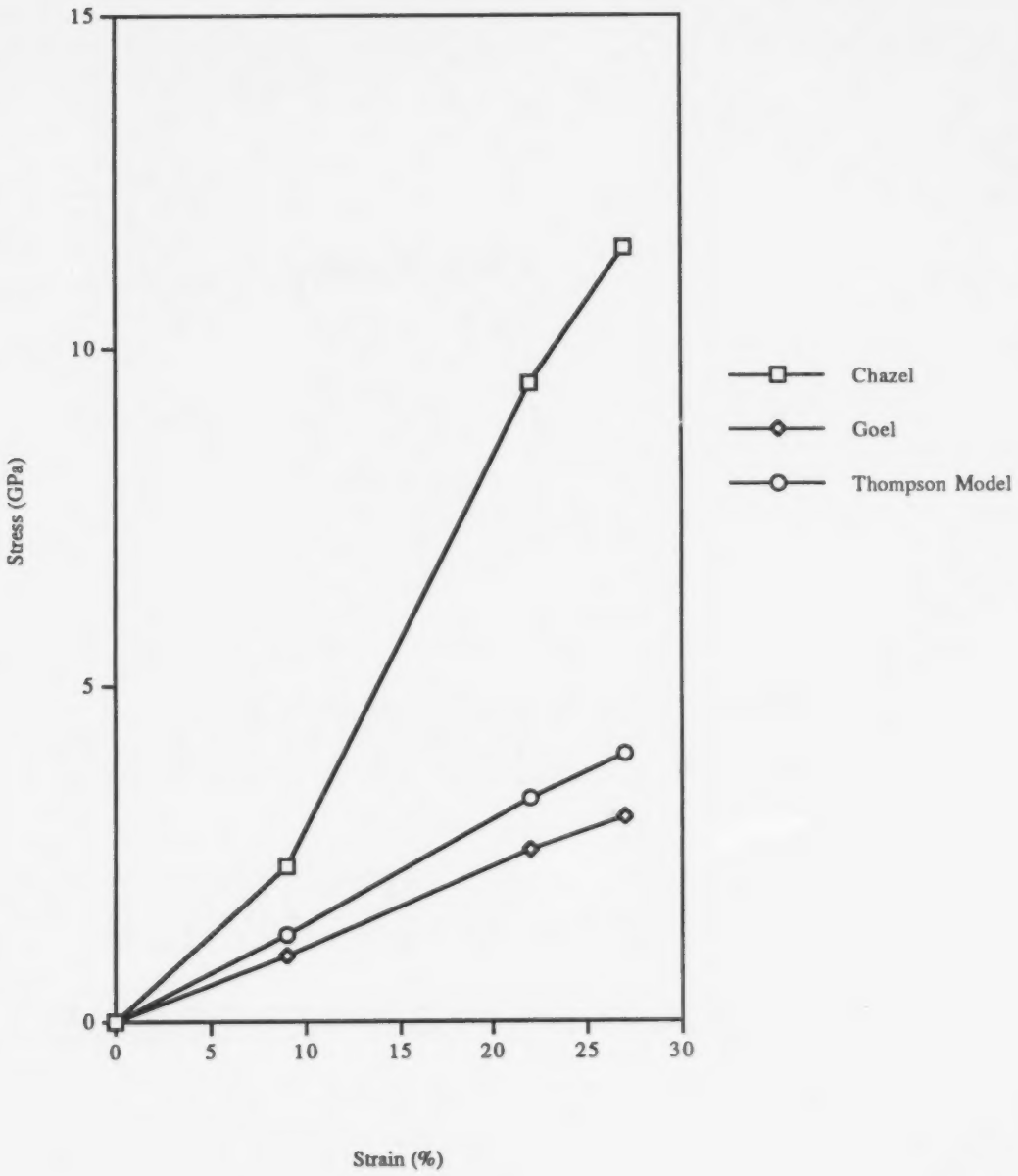

FIGURE 18: Validation of the Ligaments of the Rib-Vertebra Articulation

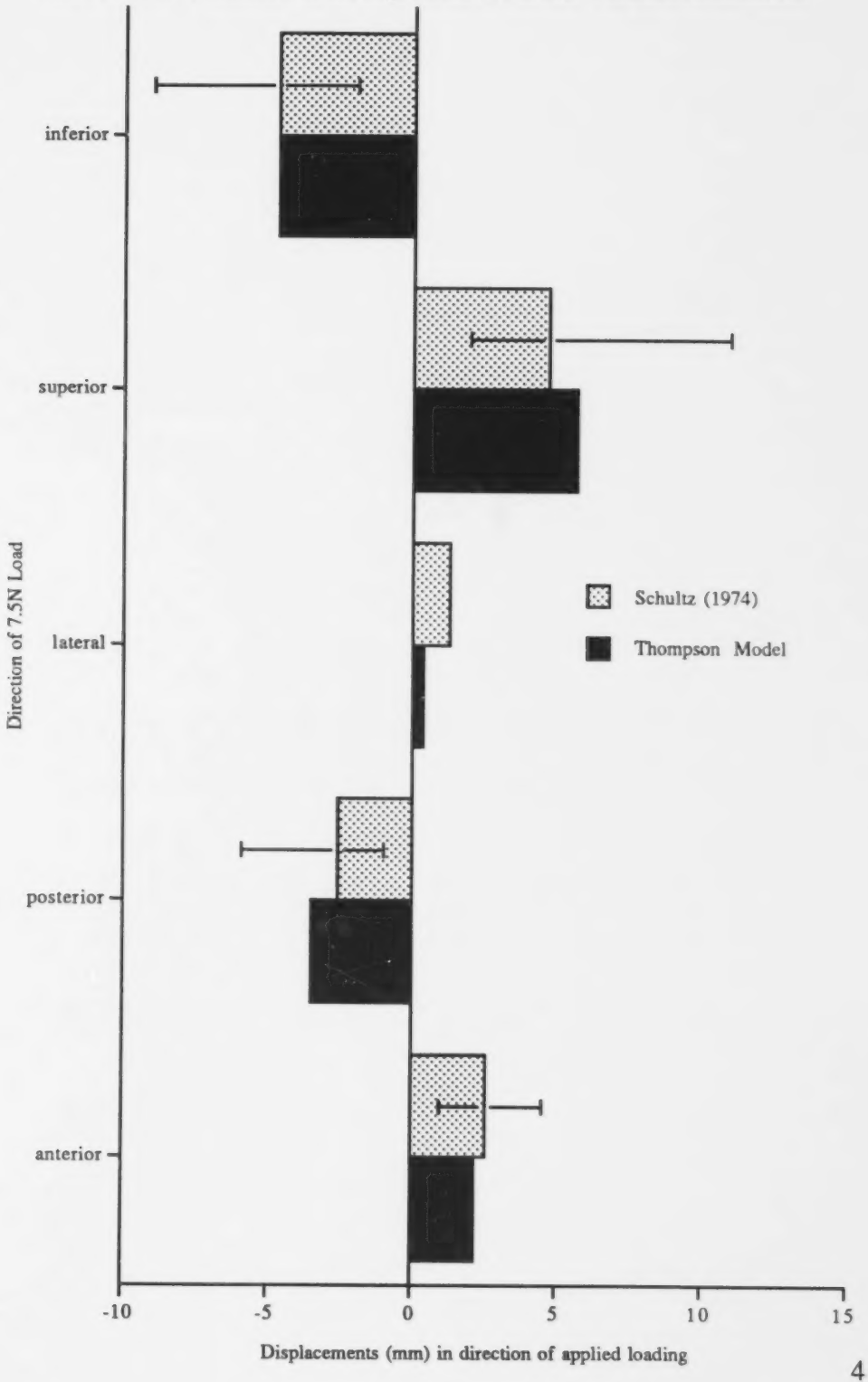

FIGURE 19: Validation of Costal Cartilage Elements

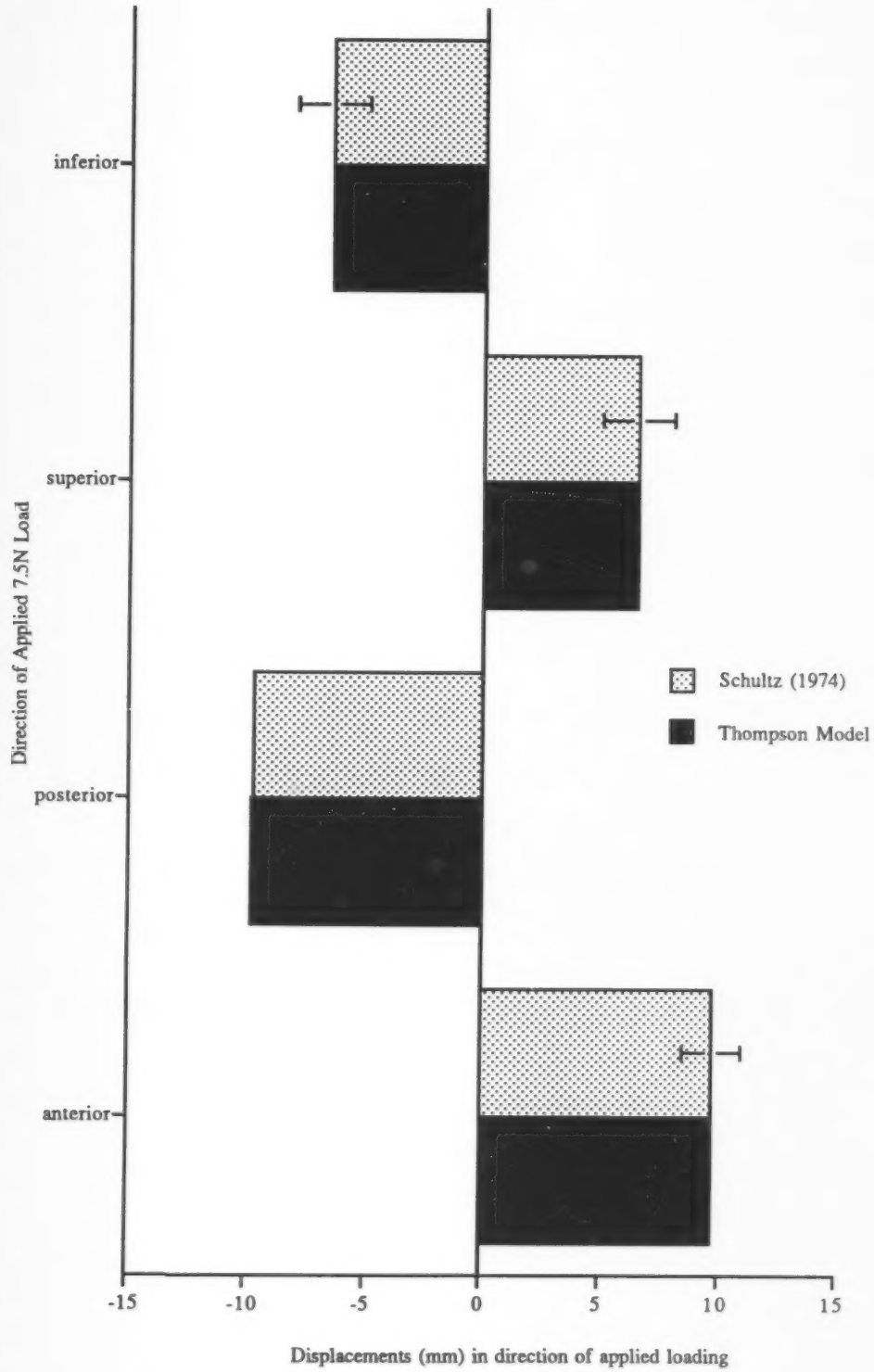

FIGURE 20: Boundary Intercostal Membranes at Physiological Length
(Side View)

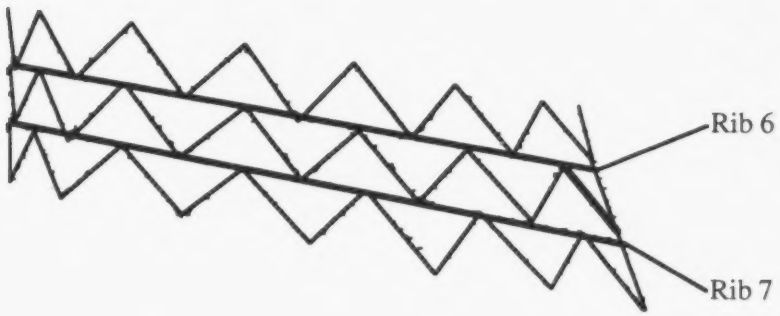

FIGURE 21: Boundary Intercostal Membranes at Extended Length
(Side View)

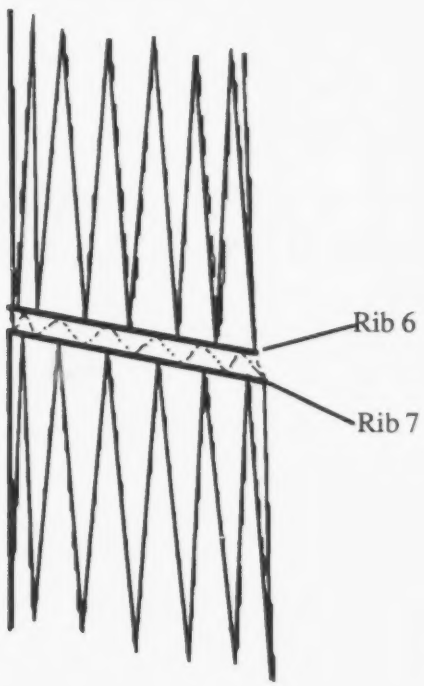

CHAPTER FOUR: RESULTS

4.0 INTRODUCTION TO CHAPTER FOUR

This chapter describes the validation study performed on the Thompson model. The validated model was then used to investigate the effects of brace loading on the rib cage. For the first run, all the element material properties and model boundary conditions were at the values specified in Chapter three. Details of the resulting displacements are included in this chapter. Next, the effects of changing both the material properties of the elements and the boundary conditions of the model were investigated. The changes in rib cage diameters, the rib displacements, and the vertebral translations and rotations for each run were recorded. These values were then compared with the output from the first, or control, run. These studies are outlined in this chapter along with figures displaying the results.

4.1 VALIDATION OF THE MODEL

In 1967, a study was performed by Agostoni investigating the deformation properties of human rib cages [1]. The subjects (three males) were seated in a specially designed steel frame with a rigid back support. Lateral squeezing forces (up to about 100 Newtons) were applied through plates positioned approximately along the midaxillary line. These loading plates were 14 centimetres high and spanned ribs two through seven. Changes in both the anterior-posterior and lateral diameters of the rib cage resulting from the applied loading were recorded using displacement transducers. Similar trials were performed on anaesthetised, paralysed subjects to validate that the conscious subjects had not resisted the squeezing forces with muscular activity.

Andriacchi et al used this study to validate their 1974 mathematical model of the rib cage [3]. Lateral forces of up to 120 Newtons were applied along the midaxillary line of ribs five through ten. No movement was permitted at the sacrum in any direction nor at T9 in the sagittal plane. They obtained good agreement between model output and experimental results. The changes in lateral diameter of their model were caused by rib rotation around the point of attachment of the vertebrae. Their model underestimated the changes in anterior-posterior diameter. Andriacchi claims this is due in part to the lack of consideration of both the intra-thoracic cavity pressure and the presence of thoracic viscera in the model.

To validate the present model, lateral squeezing forces were applied to the two ribs at the midaxillary line. The posterior surfaces of the ribs and vertebrae were constrained from motion in all directions. Two separate loading cases were applied. The first applied loads of 25, 50, and 100 Newtons respectively in accordance to the values stated by both the Agostoni and Andriacchi studies. However, since these studies applied the load over five ribs, and this model contains only two ribs, the second loading condition applied prorated loads of only 10, 20, and 40 Newtons. The lateral forces caused both rotation of the bony portions of the ribs and deformation of the costal cartilages. These movements resulted in an increase in the anterior-posterior diameter and a decrease in the lateral diameter of the rib cage.

Figure 22 is a graphical comparison of the three studies mentioned above. As can be seen from this figure, the change in lateral diameter of the present model due to the first load case (up to 100 Newtons) is in agreement with published data, while the same result due to the second or prorated load case is significantly underestimated. Furthermore, the change in anterior-posterior diameter is correctly modelled using the prorated applied loading, but significantly overestimated using the total applied loading. Instead of modelling the entire

rib cage, this study simulated the boundaries between the modelled and unmodelled components of the rib cage. This may have contributed to the discrepancies found in the validation study. It is believed that were this model expanded to represent the entire rib cage, much better agreement between Agostoni's values and the model displacements would occur.

No other experimental work was found in the literature that could be used to validate a model consisting of only three vertebrae and two ribs. However, since individual model components compare well with published experimental results (see Chapter three), the complete model is believed to display accurate physiological behaviour.

4.2 INITIAL STUDIES OF THE MODEL

Two different parametric studies were undertaken using this model. As outlined below, these focussed on changing the ligament material properties and on changing the boundary conditions while keeping the loading conditions constant. The element stiffness values were considered to be at optimum when they were assigned the values resulting from comparisons to experimental results. These stiffness values were 58.29 N/mm for the articular capsule, 19.67 N/mm for the radiate ligaments, 6.75 N/mm for the Superior Costo-transverse ligaments, and 8.33 N/mm for the other costo-transverse ligaments. The optimum values of Young's Modulus were 275 MPa for the costal cartilage and 20 MPa for the intercostal membranes. Similarly, the boundary conditions were considered to be at optimum when they are as outlined in Chapter three. These boundary conditions involve constraining T5 and T7 with intervertebral discs and constraining the ribs with the extended intercostal membranes. For the first run, all the element material properties and boundary conditions were kept at these optimum values. This is the control run. Each of the articulation ligament stiffness values, the costal cartilage and intercostal membrane element

material properties, and the boundary conditions were then independently altered from this optimum condition. Table 6 is a listing of these variations.

TABLE 6: Summary of Input Parameter Changes

Run Number	Ligament Stiffness Values	Boundary Conditions
1	all at optimum	all at optimum
2	SCT = 50 N/mm	all at optimum
3	SCT = 1.5 N/mm	all at optimum
4	CT = 50 N/mm	all at optimum
5	CT = 1.5 N/mm	all at optimum
6	Radiate = 50 N/mm	all at optimum
7	Radiate = 1.5 N/mm	all at optimum
8	Art. Capsule = 50 N/mm	all at optimum
9	Art. Capsule = 1.5 N/mm	all at optimum
10	SCT = 1000 N/mm	all at optimum
11	Art. Capsule--increase k by 5	all at optimum
12	Costal Cartilage E = 480 MPa	all at optimum
13	Intercostals E = 500 MPa	all at optimum
14	Intercostals E = 5 MPa	all at optimum
15	all at optimum	short intercostals
16	all at optimum	rigid endplates
17	all at optimum	released at sternum

4.2.1. LIGAMENT STUDY

As mentioned in section 3.2.4, the ligaments of the articulations were assigned optimum stiffness values according to the experimental work performed by Schultz *et al.* [19]. To determine the importance of accurately assigning material properties to these ligaments, the values for each set of ligaments were varied independently over the range of values reported in the literature. Stiffness values of the superior costo-transverse ligaments, the interosseous and posterior costo-transverse ligaments, the radiate ligaments, and the articular capsule ligaments were each decreased to 1.5 N/mm [24] and increased to 50 N/mm [19]. As well, the stiffnesses of the articular capsule ligaments were also increased to 5 times their original values.

4.2.2 BOUNDARY CONDITION STUDY

This study attempted to determine the optimum representation of the boundary conditions for this small scale model. Run 15 used intercostal membrane elements equal in length to the physiological distance between the ribs. This run modelled the situation in which ribs six and seven move independently from the rest of the rib pairs. Another variation of the original model involved releasing the boundary conditions at the sternum thus rendering the sternum free to move in any direction. The final variation of the boundary conditions replaced the intervertebral disc elements above T5 and below T7 with rigid constraints thereby prohibiting all movements at the superior and inferior borders of the vertebrae system.

4.3 OUTPUT PARAMETERS

In order to assess and compare the output of each run or trial, several parameters were measured and recorded. These included the changes in both lateral and anterior-posterior diameters for rib six and rib seven. Translations in all three directions of each rib both at the point of load application as well as at the vertebral end were recorded. Displacements in all three directions were also recorded for the centre front element of each of the three vertebrae. Angular displacements were also calculated to determine both the relative movement between vertebrae in the frontal plane and the absolute rotation of each vertebrae from its undeformed position in the horizontal plane.

4.4 RESULTS

4.4.1 GENERAL RESULTS

Under the previously defined loading conditions, the following results remained the same qualitatively for each run; only the magnitudes of the displacements or stresses varied. The loaded ribs experienced rigid body rotation of the bony sections as well as slight deformations of the costal cartilages. The articulation ligaments either increased or decreased in length according to their individual orientations. The vertebrae experienced two angular displacements: first, rotations in the frontal plane resulting in the intervertebral discs being more compressed on the loaded side, and second, slight rotations in the horizontal plane resulting in misalignment of the spinous processes. These vertebral angular displacements are shown in Figures 23 and 24.

The linear translations ranged from 3.4×10^{-7} mm to 0.015 mm, and the angular displacements ranged from .004 to 2.6 degrees.

The results of run 17 are not presented since releasing the constraints at the sternum produced large rigid body displacements of the ribs and sternum that are physiologically impossible.

4.4.2 LIGAMENT STUDY RESULTS

The stiffness values of each set of articulation ligaments were varied over the range of values reported in the literature. The stiffnesses of each set, the superior costo-transverse ligaments, the remaining costo-transverse ligaments, the radiate ligaments, and the articular capsules, were in turn increased to 50 N/mm and then decreased to 1.5 N/mm. The output

parameters of each of these runs were compared to the output parameters of the control run (i.e. run 1). The final results are expressed as percentage variations using the following formula:

$$\text{variation} = \frac{(\text{value of run x} - \text{value of run 1})}{\text{value of run 1}} \times 100$$

Figures 25 through 29 show the mean deviations for each of the output parameters. The rib displacements shown are the means of values from both rib six and rib seven, and the vertebral displacements are the means of values from all three vertebral levels.

4.4.3 BOUNDARY CONDITION STUDY RESULTS

The output parameters of these runs were also compared to the control run wherein the boundary conditions are as specified in Section 3.5. The results of varying the boundary conditions at the rib boundaries (i.e. decreasing the length of the intercostal fascia), at the intervertebral discs (i.e. incorporating completely restrained endplates), and at the sternum (i.e. completely unrestrained sternum) are presented in Figures 25 through 29. The method of calculating and portraying the results is the same as for the ligament stiffness study.

4.4.4 DISCUSSION OF FIGURES

Figure 25 details the changes in both the lateral and anterior-posterior diameters of the rib cage for all the runs. Only when the superior costo-transverse ligament stiffness is increased to 1000 N/mm does the variation reach a significant value. However, this change only adversely affects the anterior-posterior diameter and not the lateral diameter. Both diameters are affected the most by changes in the boundary conditions and in the material properties of the intercostal membrane and costal cartilage elements.

Rib displacements in all three directions at the point of load application are shown in Figure 26. The z-direction displacements are the most significant, especially when the Young's Modulus of the intercostal membrane elements is decreased by 75%. The same is true for the rib displacements at the costo-vertebral junction as shown in Figure 27. This figure also demonstrates the significant effect of varying the boundary conditions of the vertebrae on these rib head displacements.

Figure 28 illustrates the variations in the translations that occur at the centre front elements of the vertebrae. As to be expected, imposing a fixed constraint on T5 and T7 results in large discrepancies in vertebral body displacements when compared to the control run. The intercostal membrane boundary condition also significantly affects these displacements. The horizontal and frontal plane angular displacements of the vertebrae are shown in Figure 29. These rotations are adversely affected only by changing the boundary conditions of the vertebrae.

FIGURE 22: Validation of Model

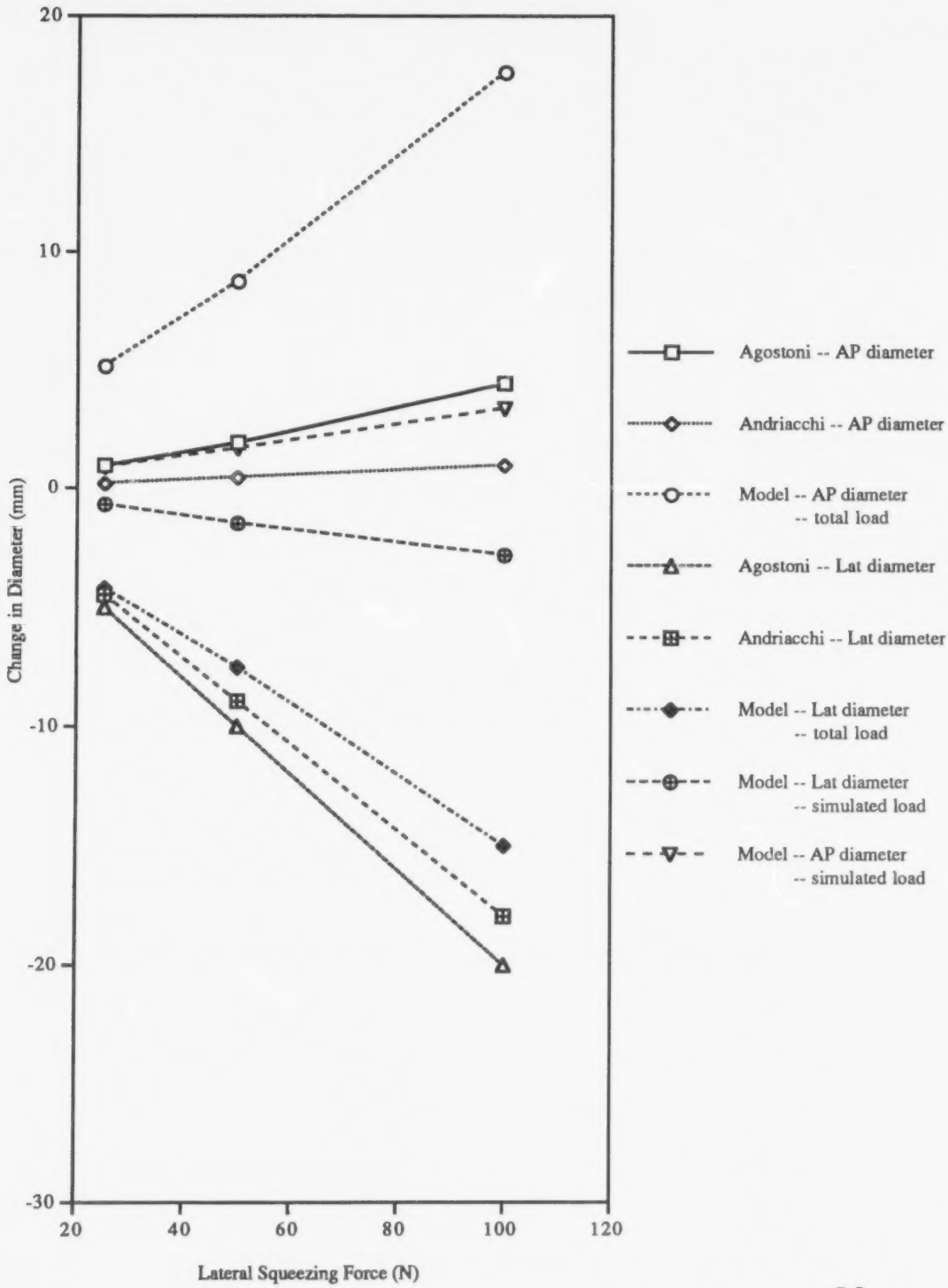

FIGURE 23: Vertebral Rotations in the Frontal Plane Due to Brace Loading
(Displacements are not to scale)

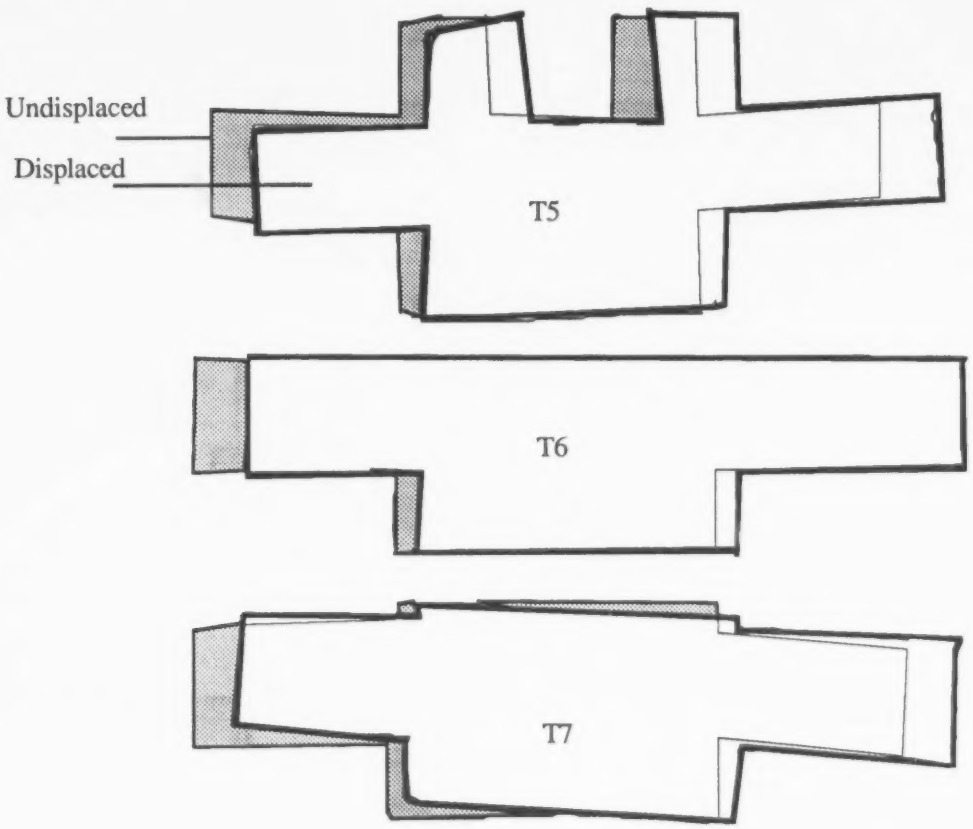

FIGURE 24: Vertebral Rotations in the Horizontal Plane Due to Brace Loading
(Displacements are not to scale)

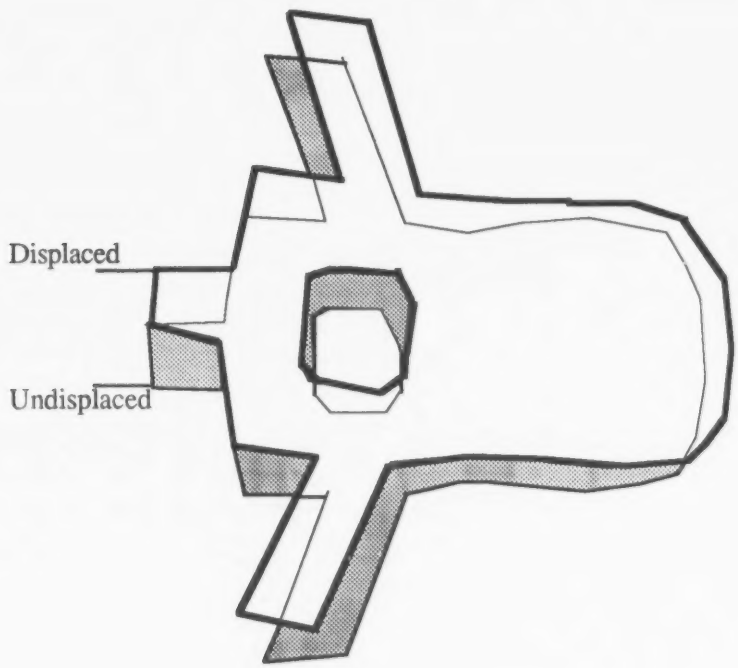

FIGURE 25: Changes in Rib Cage Diameters

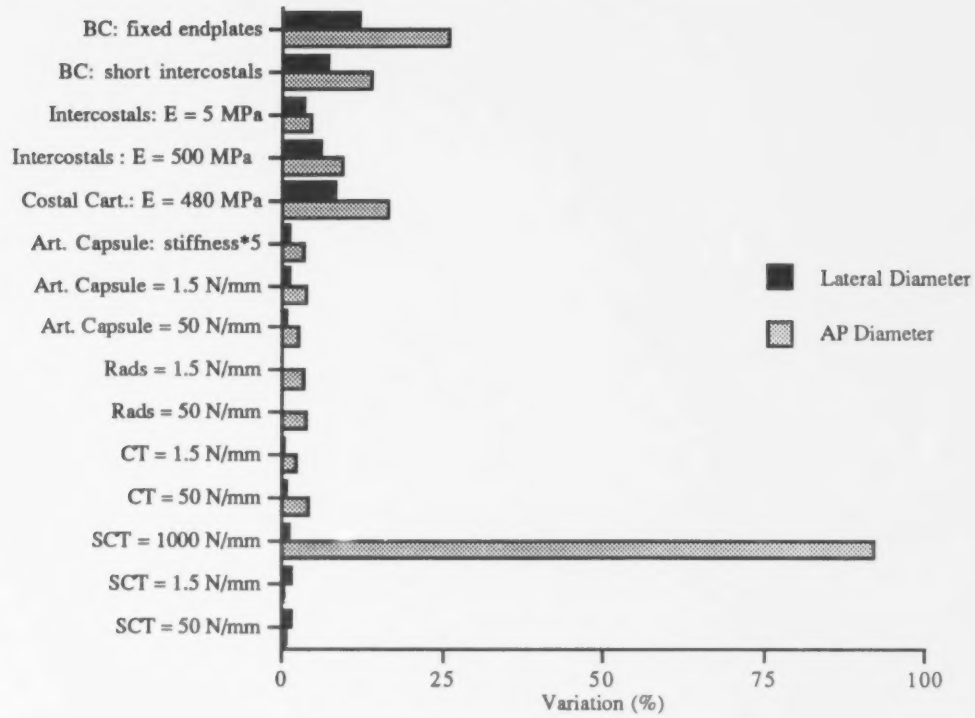

FIGURE 26: Rib Displacements at the Point of Load Application

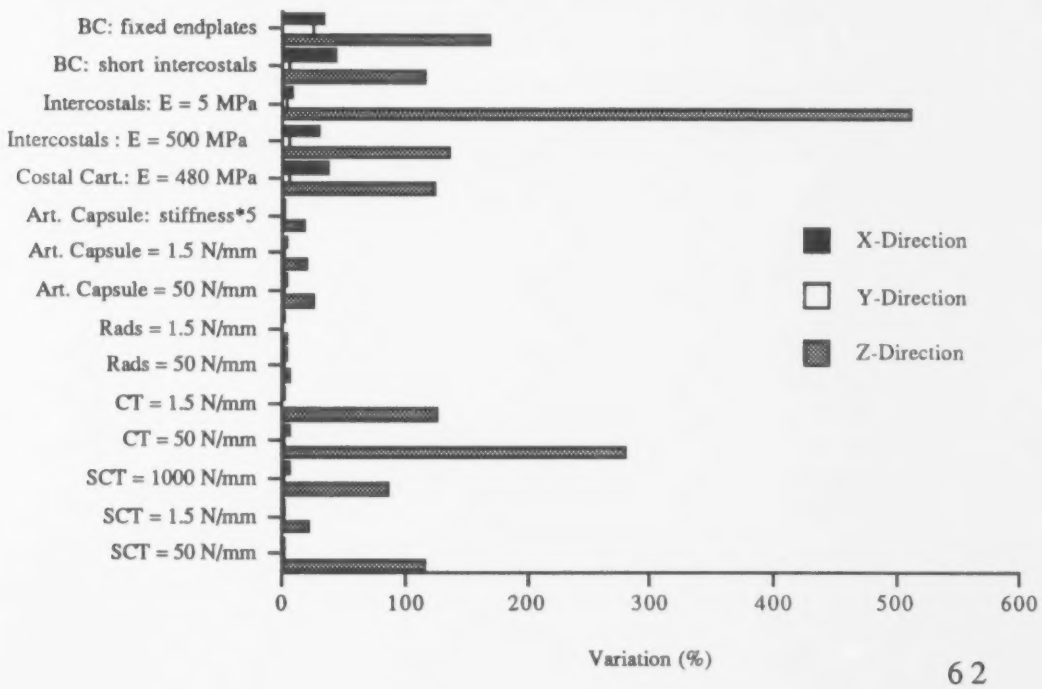

FIGURE 27: Rib Displacements at the Costo-vertebral Junction

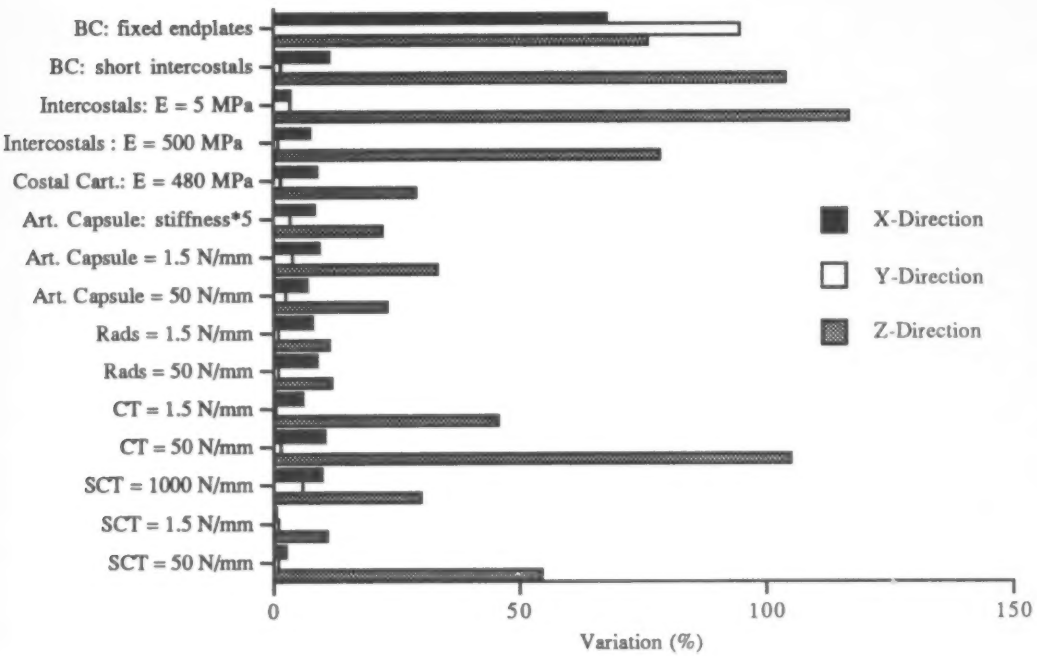

FIGURE 28: Displacements of the Vertebrae

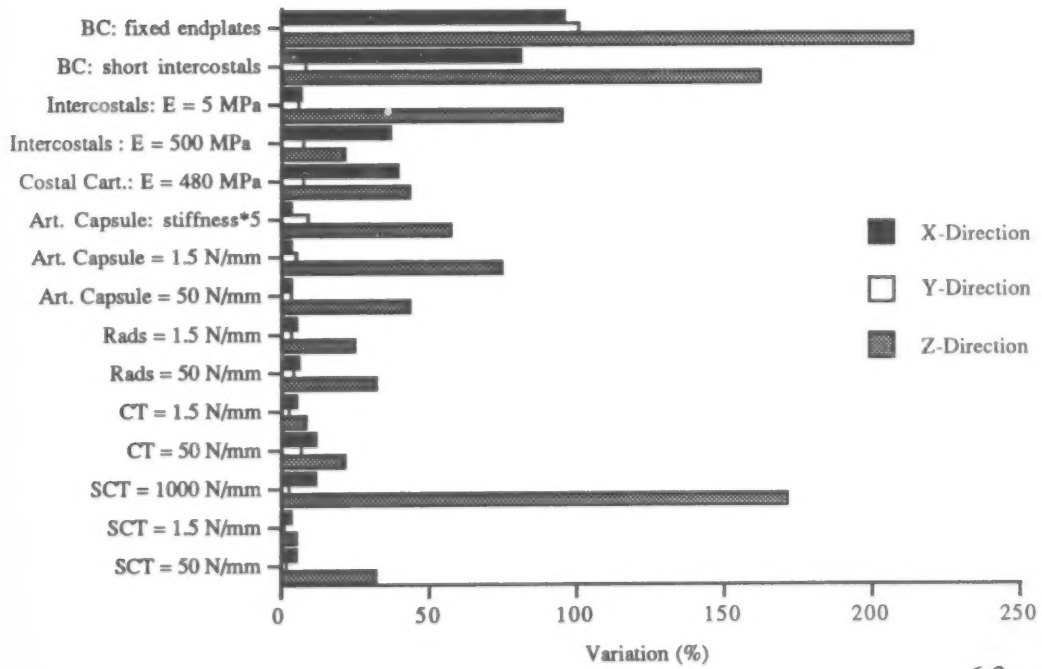

FIGURE 29: Vertebral Rotations

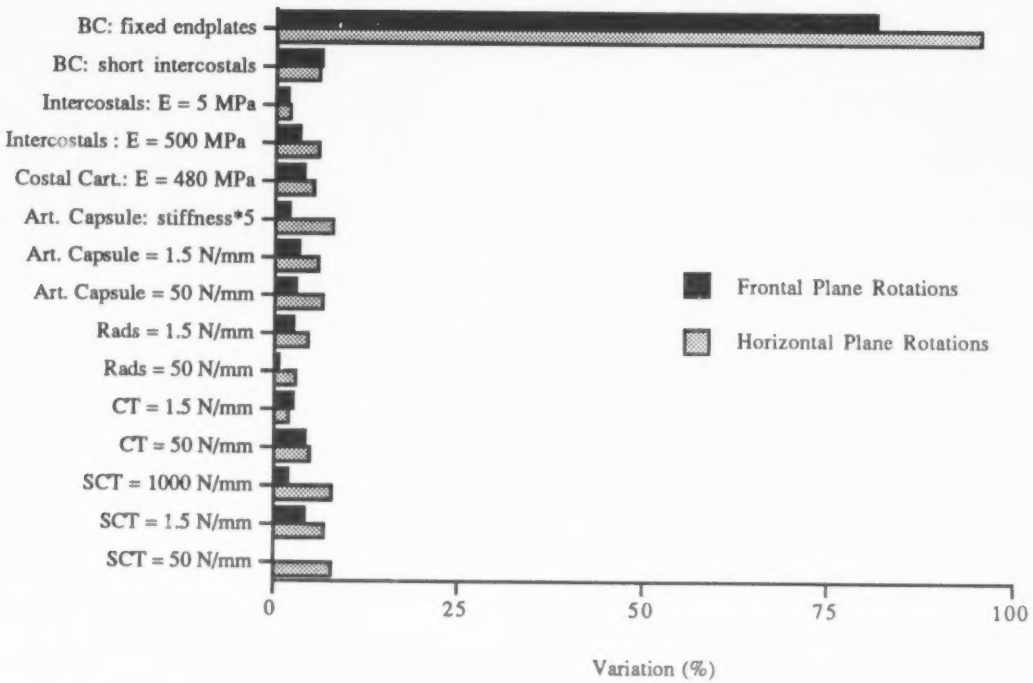

CHAPTER FIVE: DISCUSSION OF RESULTS

5.0 GENERAL QUALITATIVE RESULTS

This study does not attempt to quantify the effects of bracing on the rib cage. Rather, this study attempts to discover several qualitative results of bracing as well as investigating the effects of changes in element properties and boundary conditions in the finite element model. Under the applied loading conditions several general output characteristics were observed.

Although biological tissues are viscoelastic, the displacements experienced by this elastic model are small enough to accurately portray the physiological movements of the spine and rib cage. The loading condition, which simulates a scoliosis brace, when applied to a normal spinal alignment results in slight horizontal translations of the vertebrae with accompanying angular displacements. Since these are desirable movements in scoliosis correction, it may then be assumed that if the same loading were applied to a scoliotic spine, a reduction in the spinal deformity would occur. Also, during the course of the parametric study of the model components, the model output was as expected in that an increase in ligament stiffness values resulted in smaller movements of the ribs and vertebrae, and a decrease in ligament stiffness values resulted in larger movements.

By investigating the results displayed in Figures 25 through 29 several conclusions were drawn concerning the effects of brace forces on the human thorax and the transmission of these forces through the ribs to the spine. As well, these figures demonstrated the effects of varying the element stiffness values and the boundary conditions on the model output.

5.1 PARAMETRIC STUDY

5.1.1 ARTICULATION LIGAMENTS

Runs two through eleven focus on varying the stiffness values of the articulation ligaments. All of these runs share some common output characteristics. Most of the rib displacements show no significant deviation from the control values. These displacements demonstrate a variation range of 0.0% to 11.3% when compared to the control run. Likewise, the deviations of both the linear and angular vertebral displacements generally range from 0.0% to 11.5%. These small variations in output values suggest that the articulation ligaments may be assigned stiffness values ranging from 1.5 N/mm to 50 N/mm as published in previous studies. In fact, only in run four, when the superior costo-transverse ligament is assumed to exhibit the mechanical behaviour of pure collagen (i.e.. a stiffness value of 1000 N/mm), do the percentage variations show any significant increase, with a mean value of 20.9% (ranging from 0.2% to 171.6%).

However, there are some exceptions to the above values. The z-direction displacements, both for the ribs and the vertebrae, have a higher percentage deviation range of 1.0% to 279.6% when compared to the control run. It is believed that if the simulated boundary conditions between the model components and their adjacent counterparts which were not included were more physiologically correct, these deviations would be less significant.

Table 7 shows the mean values of the percentage variations for each of the ligament study runs, excluding the exceptions mentioned above. The small range of mean values for these runs, between 2.3% and 4.9%, indicates that the ligament stiffness values may be varied over a large range without adverse effects on model output. This suggests that a simpler model of the rib-vertebra articulation involving fewer elements would be feasible.

TABLE 7: Percentage Variations for the Ligament Study (mean values)

Run:	2	3	4	5	6	7	8	9	10	11
Mean %:	2.9	2.5	4.7	2.3	2.3	3.1	3.3	4.2	4.9	3.5

Scoliotic bracing treats the deformity by attempting to derotate and realign the vertebrae. Because of this, one measurement of the effectiveness of the brace is the amount of vertebral displacements, both linear and angular. From Figure 29, it can be seen that the superior costo-transverse ligament has the greatest effect on spinous process alignment (i.e. angular displacements in the horizontal plane), and that the other costo-transverse ligaments have the greatest effects on vertebral body alignment (i.e. angular displacements in the frontal plane). It is the costo-transverse ligaments, along with the radiate ligaments of the costo-vertebral articulations, which contribute the most to horizontal displacements of the vertebrae, as shown in Figure 28.

5.1.2 COSTAL CARTILAGE

When the Young's Modulus for the costal cartilage elements was increased from 275 MPa to 480 MPa, the deviations in the output parameters as compared to the control run varied from 0.0% to 124.3% (mean value = 9.8%). As the costal cartilage stiffened, its ability to deform decreased, resulting in a substantial lowering of rib displacement values. It is worth noting that, for this run, changes in both lateral and anterior-posterior diameters of the rib cage, as shown in Figure 25, were decreased by a mean value of 12.3%. These same parameters only experienced a mean deviation of 1.6% for the articulation ligament runs. This reinforces the belief that changes in rib cage diameters occur mostly due to deformations of the costal cartilage which allow for rotations of the bony sections of the ribs.

5.1.3 INTERCOSTAL MEMBRANES

Runs 13 and 14 study the effects of increasing and decreasing the stiffness of the intercostal membrane elements. The output from these runs is significantly different than the control values. The percentage variations of the output parameters in these two runs range from 0.3% to 512.8% with a mean value of 31.1%. Clearly, inaccurate modelling of these membranes will lead to incorrect model output. However, assigning physiologically correct material properties to the intercostal membranes is difficult as there is insufficient data available which details the mechanical behaviour of these membranes. Also the following section will demonstrate that this limitation in modelling the intercostal membranes hinders their effectiveness in acting as boundary constraints for the ribs.

5.2 BOUNDARY CONDITION STUDY

The large variations occurring in runs 15 and 16 clearly underline the importance of accurate simulation of boundary conditions in the model. When the boundary intercostal membrane elements are shortened to the length of intercostal spaces, deviations in the range of 0.3% to 162.7% (mean = 27.6%) are incurred. When the boundary intervertebral discs are removed and the superior endplate of T5 and the inferior endplate of T7 are constrained from any movements, the output values experience variations ranging from 0.1% to 214.1% with a mean value of 38.6%, when compared to the control run.

Neither of these runs is physiologically correct. The endplates of the vertebrae are not rigidly fixed as assumed in run 16, but rather they are constrained by the adjacent intervertebral discs and vertebrae, the soft tissues of the spine (i.e.. muscles and ligaments), and the attached ribs. As well, in run 15, when the lengths of the elements representing the intercostal membranes were made equal to the physiological distance

between ribs five and six, the axial forces incurred under the applied loading were greater than 3 Newtons. This indicates that the situation being modelled is one in which only ribs six and seven are responding to the loading conditions while the rest of the ribs remain stationary. Obviously, due to the complex interactions between all the components in the rib cage, this is physiologically impossible.

CHAPTER SIX: LIMITATIONS AND FUTURE WORK

6.0 CONCLUSIONS

The following conclusions may be drawn from the results of this study:

1. The superior costo-transverse ligament contributes the most to the amount of vertebral rotation about the z-axis. The posterior and interosseous costo-transverse ligaments, along with the radiate ligaments, have the greatest effect on the stability of the vertebral bodies. Angular displacements of the vertebrae in the frontal plane are controlled mostly by the posterior and interosseous costo-transverse ligaments.

2. The brace forces, which attempt to reduce the spinal curvature and derotate the vertebrae, producethe desired movements of the rib cage components.

3. The stiffness values of the articulation ligaments may be varied over the range reported in previously published studies without adversely affecting the output of the model. Stiffness variations of the costal cartilage elements lead to significant changes in the displacements of the ribs and vertebrae. It is therefore important to accurately assign material properties to these elements.

4. The output parameters are highly sensitive to changes in both the length and the stiffness values of the intercostal membranes. Accurate material property data must be used to model these elements correctly. Physiologically accurate boundary conditions are essential in order to obtain reliable model output. A complete model of the entire thorax should be designed to obtain quantitatively correct results.

6.1 MODEL LIMITATIONS

The greatest limiting factor on the accuracy of this model is the lack of experimental data available. Detailed descriptions of the spatial orientation of the various ligaments associated with the rib-vertebra articulation, as well as sufficient experimental work describing the mechanical properties of each individual ligament, would allow a more physiologically correct model to be designed and constructed. A lack of data describing the mechanical characteristics of the intercostal membranes also contributes to inaccuracies in model output.

A further limitation of this model is due to the software package utilised. A robust finite-element analysis package that allows both geometric and material non-linearities in a complex model would more accurately simulate the biomechanical behaviour of soft tissues such as the ligaments and the intervertebral discs. The use of gap elements that are active only in compression would best model the articular facets of the spine and the points of bone-to-bone contact at the costo-vertebral and costo-transverse articulations.

Although this model provides information about the rib-vertebra articulation, as well as a qualitative look at rib and vertebra movement under loading, it does not provide information about the reaction of the entire thorax to applied scoliosis bracing. The boundary conditions imposed on this small scale model fail in the attempt to replicate those found between the components of the rib cage in true physiological conditions. The most insufficient applied boundary condition occurs at the sternum. In the body, the sternum is neither rigidly fixed (i.e. no translations or rotations allowed) nor is it completely unrestrained from motion. Rather, the movement of the sternum is constrained by the attachment of the remaining five pairs of ribs not included in this model. A more accurate

boundary condition for this small scale model would be to restrain the sternum with spring elements representing the stiffness values of these ribs and their subsequent attachments to the spinal column.

6.2 FUTURE WORK

This model is only a preliminary study of the effects of bracing on the spine and rib cage. In order to better understand the complex interactions between the brace and the body during scoliosis treatment, this small-scale model needs to be expanded to represent the entire human thorax. In order to produce a more feasible, complete rib cage model, the number of elements involved in modelling the rib-vertebra articulations needs to be reduced while still ensuring accurate model output. The results from the Thompson model could be used to test the validity of replacing the four sets of articulation ligaments, comprised of 13 truss elements, with only two truss elements. The stiffness values for these elements could be an average of the values used in this model. One truss could be located between the rib tubercle and the transverse process, and the other between the rib head and the vertebral body. An iterative method could be used to determine the optimum placement of these truss elements.

Furthermore, to more accurately model a complete physiological system, use of a non-linear finite element analysis package is necessary. Using this package, the ligament elements could be designed to act in tension only. Successful modelling of the bone-to-bone contact with gap elements that are active in compression only would also be an improvement.

Every model, however, will be limited by the lack of data outlining correct geometrical placement and mechanical behaviour of the model components. More experimental work

needs to be performed in order to evaluate these characteristics. The work performed previously on the ribs and the rib-vertebra articulations [18,19] should be redone with more sophisticated testing methods and measuring devices. Tensile tests to determine the properties of spinal and articulation ligaments should also be undertaken. These tests should attempt to test isolated ligaments, interactions between sets of ligaments, and behaviour of the entire rib-vertebra joints.

A further study could also be performed to investigate a wider variety of geometrical changes of the spine and rib cage due to the scoliosis condition. Use of a computer program to alter the geometry of the individual components of the model would simplify this procedure. This program would allow the user to change the spinal curvature, the individual vertebral rotations, and the lengths and the widths of the components of each vertebra. The program would then modify the geometry of the remaining model components accordingly.

Once this global model is complete, it may then be used as a powerful tool in researching both the etiology and the treatment of scoliosis. When used in a clinical setting, the model would help to determine the optimum placement of the pressure pads within the brace. Moreover, studies could be performed which investigate different theories concerning the initiation of scoliosis. For example, an investigation of asymmetrical growth as a cause of scoliosis could be undertaken and the results compared to a similar study published by Stokes and Laible [22]. A further modification of the model would be to incorporate the time-dependent behaviour of biological tissues in order to look at the long-term effects of bracing.

REFERENCES

1. Agostoni E., Mognoni P., Torri G., Miserocchi G. (1966) Forces Deforming the Rib Cage. *Resp. Physiol.* **2**, 105-117.

2. Algor, Inc. (1993) *Algor Reference Manuals*. Algor, Inc. Pittsburgh, Pa.

3. Andriacchi T. P., Schultz A. B., Belytschko T. B., Galante J. O. (1974) A Model for Studies of Mechanical Interaction between the Human Spine and Ribcage. *J. Biomechanics* **7**, 497.

4. Blout W. P., Moe J. H. (1980) *The Milwaukee Brace*. Williams & Wilkins Company, Baltimore, MD.

5. Chazel J., Tanguy A., Bourges M., Gaurel G., Excande G., Buillot M., Vanneuville G. (1985) Biomechanical Properties of Spinal Ligaments and a Histological Study of the Supraspinal Ligament in Traction. *J. Biomechanics* **18**, 167-176.

6. Closkey R. F., Schultz A. B., Luchies C. W. (1993) A Model for Studies of the Deformable Rib Cage. *J. Biomechanics* **25**, 529-539.

7. Dansereau J. and Stokes I. A. F. (1988) Measurements of the Three-Dimensional Shape of the Rib Cage. *J. Biomechanics* **21**, 893-901.

8. Dumas G.A. (1994) Some Geometrical Parameters of Spinal Facets. Personal correspondence.

9. Fung Y.C. (1981) *Biomechanics: Mechanical Properties of Living Tissues*. Springer-Verlag, USA.

10. Goel V. K., Kong W., Han J. S., Weinstein J. N., Gilbertson L. G. (1993) A Combined Finite Element and Optimisation Investigation of Lumbar Spine Mechanics with and without Muscles. *Spine* **18**, 1531-1541.

11. Gray H. (C. M. Goss (Ed)) (1976) *Anatomy of the Human Body*. Lea and Febiger, Philadelphia, PA.

12. Kapandji I. A. (1970) *The Physiology of the Joints (Vol. 3)*. Churchill Livingstone, USA.

13. Panjabi M., Takata K., Goel V., Federico D., Oxland T., Duranceau J., Krag M. (1991) Thoracic Human Vertebrae: Quantitative Three-Dimensional Anatomy. *Spine* **16**, 888-901.

14. Panjabi M. *et al.* (1976) Three-dimensional Flexibility and Stiffness Properties of the Human Thoracic Spine. *J. Biomechanics* **9**, 185-192.

15. Raso V. J., *et al* . (1992) A Biomechanical Analysis of the Effect of Boston Brace Forces on the Spine. Presented to the 9th Combined Meeting of the Orthopaedic Association of the English Speaking World, Toronto, Canada.

16. Roberts S. B., Chen P. H. (1970) Elastostatic Analysis of the Human Thoracic Skeleton. *J. Biomechanics* **3**, 527-545.

17. Schultz A. B., Belytschko T., Andriacchi T. P., Galante J. O. (1973) Analog Studies of Forces in the Human Spine: Mechanical Properties and Motion Segment Behaviour. *J. Biomechanics* **6**, 373.

18. Schultz A. B, Benson D., Hirsch C. (1974a) Force-Deformation Properties of Human Ribs. *J. Biomechanics* **7**, 303-309.

19. Schultz A. B, Benson D., Hirsch C. (1974b) Force-Deformation Properties of Human Costo-Sternal and Costo-Vertebral Articulations. *J. Biomechanics* **7**, 311-318.

20. Shute R. D. (1993) Finite Element Model of a Spinal Motion Segment. Internal Report (Glenrose Rehabilitation Hospital).

21. Shute R. D. (1994) A Finite Element Model of the Thoracic Spine and Rib Cage. Internal Report (Glenrose Rehabilitation Hospital).

22. Stokes I. A. F. and Laible J. P. (1988) Three-dimensional Osseo-ligamentous Model of the Thorax Representing Initiation of Scoliosis by Asymmetric Growth. *J. Biomechanics* **21**, 893-901.

23. Sundaram S. H. and Feng C. C. (1977) Finite Element Analysis of the Human Thorax. *J. Biomechanics* **10**, 505-516.

24. White A. A. and Panjabi M. M. (1978) *Clinical Biomechanics of the Spine.* J. B. Lippincott, Philadelphia, PA.